AD NUMBER: AD0293830

LIMITATION CHANGES

TO:

Approved for public release; distribution is unlimited.

FROM:

Distribution authorized to U.S. Gov't. agencies and their contractors; Administrative/Operational Use; 1 Oct 1962. Other requests shall be referred to the Aeronautical Systems Division, Flight Dynamics Lab, Wright-Patterson AFB, OH 45433.

AUTHORITY

10 FEB 1965, per SEG Ltr 10 FEB 1965

AD 293 830

THERMAL STRESSES AND DEFLECTIONS IN RECTANGULAR PANELS PART II - THE ANALYSIS OF RECTANGULAR PANELS WITH THREE-DIMENSIONAL HEAT INPUTS

TECHNICAL REPORT NO. ASD-TR-61-537, PT. II

October 1962

Flight Dynamics Laboratory
Aeronautical Systems Division
Air Force Systems Command
Wright-Patterson Air Force Base, Ohio

Project No. 1467, Task No. 146702

(Prepared under Contract No. AF33(616)-7751 by Republic Aviation Corporation, Farmingdale, L.I., N. Y.; M. Newman and M. J. Forray, authors)

NOTICES

When Government drawings, specifications, or other data are used for any purpose other than in connection with a definitely related Government procurement operation, the United States Government thereby incurs no responsibility nor any obligation whatsoever; and the fact that the Government may have formulated, furnished, or in any way supplied the said drawings, specifications, or other data, is not to be regarded by implication or otherwise as in any manner licensing the holder or any other person or corporation, or conveying any rights or permission to manufacture, use, or sell any patented invention that may in any way be related thereto.

* * *

ASTIA releases to OTS not authorized.

* * *

Qualified requesters may obtain copies of this report from the Armed Services Technical Information Agency, (ASTIA), Arlington Hall Station, Arlington 12, Virginia.

* * *

This report shall not be considered as an endorsement of any item. The report shall not be used for advertising purposes by any organization.

* * *

Copies of ASD Technical Reports and Technical Notes should not be returned to the Aeronautical Systems Division unless return is required by security considerations, contractual obligations, or notice on a specific document.

FOREWORD

This report was prepared by the Republic Aviation Corporation under USAF Contract No. AF 33(616)-7751. This contract was sponsored by Technical Area 750A, "Mechanics of Flight." The work was begun under Project 1367, Task 14002. The work was completed under Project 1467, "Structural Analysis Methods," Task 146702, "Thermoelastic Structural Analysis Methods." The work was administered under the Flight Dynamics Laboratory, Deputy Commander/Technology, Aeronautical Systems Division, with Mr. G. E. Maddux acting as Project Engineer.

The analyses were performed by Dr. Malcolm Newman and Dr. Marvin Forray of the Structural Research and Development Group, Structures Section, Paul Moore Research and Development Center. Numerical analysis and programming were performed by Sidney Kalman, Saul Serben, Bernard Sackaroff, and Harold Schechter under the supervision of Morris Gershinsky Norman Levine of the Digital Computing Division.

A separate report containing a detailed description of the computer program has been prepared. This report includes input instructions, flow charts, a description of the pertinent format, and all other information required to perform the analysis on an IBM 7090 computer. A copy of this report may be obtained by contacting the Flight Dynamics Laboratory, ASRMDS-22.

The entire program was coordinated and supervised by Dr. Robert S. Levy, Head of the Structural Research and Development Group. The value of his active participation is gratefully acknowledged, as well as the helpful assistance of Mr. A. Alberi, Manager of Technical Engineering, and Mr. C. Rosenkranz, Acting Chief of Structures of the Paul Moore Research and Development Center.

This report was issued by Republic Aviation Corporation as Report RAC 548-1 (ARD-688-7).

This report is the final report on this contract.

ABSTRACT

The linear thermal stress problem of a rectangular plate subjected to arbitrary three-dimensional heating is solved. Analytic solutions for the determination of deflections and stresses are presented for several types of boundary conditions. A digital computer program is developed which, starting with heat transfer, material, and geometry data, yields a numerical evaluation of transient temperatures, quasi-static deflections, and stresses. A copy of this report may be obtained by contacting the Flight Dynamics Laboratory, ASRMDS-22.

PUBLICATION REVIEW

This report has been reviewed and approved.

FOR THE COMMANDER:

RICHARD F. HOENER
Chief, Structures Branch
Flight Dynamics Laboratory

TABLE OF CONTENTS

LIST OF ILLUSTRATIONS

NOMENCLATURE

a, b	Plate planform dimensions
c	Specific heat
D	Plate flexural rigidity = $\frac{Eh^3}{12(1-\nu^2)}$
E	Young's modulus
h	Plate thickness
K	Thermal conductivity
M_x, M_y	Bending moments per unit of length acting on sections perpendicular to the x and y axes, respectively
$\overline{M}_x$, $\overline{M}_y$	$\frac{M_x b^2}{Dh}$, $\frac{M_y b^2}{Dh}$, respectively - nondimensional bending moments
M_{xy}	Twisting moment per unit of length
$\overline{M}_{xy}$	$\frac{M_{xy} b^2}{Dh}$ - Nondimensional twisting moments
M_T	$E \int_{-\frac{h}{2}}^{\frac{h}{2}} \alpha T z \, dz$
$\overline{M}_T$	$\frac{M_T b^2}{D(1-\nu)h}$
N_T	$E \int_{-\frac{h}{2}}^{\frac{h}{2}} \alpha T \, dz$
$\overline{N}_T$	$\frac{N_T b}{Eh^2}$

N_x, N_y	Resultant forces per unit of length in the y and x directions, respectively
$\overline{N}_x$, $\overline{N}_y$	$\frac{b(1-\nu)N_x}{Eh^2}$, $\frac{b(1-\nu)N_y}{Eh^2}$, respectively - nondimensional resultant forces
N_{xy}	Resultant shearing force per unit length in the xy plane
$\overline{N}_{xy}$	$\frac{2b(1+\nu)N_{xy}}{Eh^2}$ - nondimensional resultant shearing force
q	Distributed external load per unit of planform area
Q_x, Q_y	Transverse shearing forces per unit of length in the y and x directions, respectively
S	Heat flux to surface
t	Time
T	Local temperature change from that of an initial unstressed state
T_w	Adiabatic wall temperature
u, v	Displacements in the x and y directions, respectively
w	Deflection
$\overline{w}$	$\frac{w}{h}$
x, y	Planform rectangular coordinates
z	Thickness coordinate
α	Coefficient of linear thermal expansion
γ_{xy}	Shearing strain in the xy plane
ϵ	Emissivity
ϵ_x, ϵ_y	Direct strains in the x and y directions, respectively
λ	$\frac{a}{b}$
ν	Poisson's ratio
ϕ	Stress function
ρ	Mass density
σ	Stefan-Boltzmann constant

$\sigma_x, \sigma_y, \sigma_z$	Stresses in the x, y, and z directions, respectively
$\sigma_{xy}, \sigma_{yz}, \sigma_{zx}$	Shearing stress in the xy, yz,and zx planes, respectively
ξ, η	$\frac{x}{a}$ and $\frac{y}{b}$, respectively
o	Superscript - Refers to midplane

SECTION I - INTRODUCTION

In Part I of this study (Reference 1) an analysis was presented for the determination of the bending deflections and stresses in rectangular plates subjected to temperatures which varied through the thickness only. The present work is an extended, more comprehensive analysis which accommodates three-dimensional heating, i.e., where the temperatures are time-dependent and vary arbitrarily over the planform and through the thickness.

Attention is restricted to Fourier heat conduction problems, and the analysis employs classical plate theory. This permits the uncoupling of membrane and bending effects so that the stress analysis problem may be divided into the following superposable parts.

(1) An "in-plane" problem in which the plate experiences only in-plane force resultants (membrane forces) and displacement components.

(2) A "bending" problem in which deflections normal to the undeflected midplane occur (without stretching), producing bending and twisting moments but no membrane forces.

For the in-plane problems, the following boundary conditions are treated:

Case I: Immovable edges - Displacements normal to and along the edges are prevented.

Case II: Edges unrestrained tangentially but normally immovable - Points on the plate edge can move freely in the direction of the edge (freely sliding), but are restrained against motion normal to the edge. This situation occurs when the plate is inserted into, but not mechanically fastened to, a frictionless, rigid frame.

Case III: Free plate - No forces at the edges.

The following bending problems are accommodated:

Case IV: Clamped plate - No deflections or rotations at the plate edges.

Case V: Simply supported edges - No deflections but free rotations at the boundary.

The complete stress analysis problem is defined when one of the in-plane cases (I, II, or III) is coupled with one of the bending cases (IV or V). The total stresses are then obtained by superposing the sets of stresses resulting in each case.

In order to automate the numerical analysis, a heat transfer program (described more fully in Section V-A) was written and then integrated with the stress analysis. This integration resulted in a general digital computer program which, based on heat transfer, material, and geometry input data, permits the determination of time-dependent temperatures, quasi-static deflections (i.e., neglecting dynamic effects), and stresses.

The major emphasis in this study was the analytical development pertaining to the thermal stress analysis. Thus, Sections II, III, and IV present the basic stress analysis equations and their solutions. The heat transfer equations, however, were solved numerically rather than analytically by a finite difference procedure.

Manuscript released by the authors 29 October 1962 for publication as an ASD Technical Report.

SECTION II - FUNDAMENTAL STRESS ANALYSIS EQUATIONS

A. STRESS-STRAIN-DISPLACEMENT RELATIONS

The plate (see Figure 1) is referred to a Cartesian, xyz coordinate system with the origin at one corner of the midplane. If plane sections are assumed to remain plane and normal to the deflected middle surface, the x and y components of displacement are

$$u = u^o(x,y) - z\frac{\partial w}{\partial x}$$
$$v = v^o(x,y) - z\frac{\partial w}{\partial y} \qquad (1)$$

where u^o, v^o are the x, y components of midplane displacements and $w = w(x,y)$ is the displacement in the z direction. The strains are then given by

$$\epsilon_x = \epsilon_x^o - z\frac{\partial^2 w}{\partial x^2}$$
$$\epsilon_y = \epsilon_y^o - z\frac{\partial^2 w}{\partial y^2} \qquad (2)$$
$$\gamma_{xy} = \gamma_{xy}^o - 2z\frac{\partial^2 w}{\partial x \partial y}$$

where

$$\epsilon_x^o = \frac{\partial u^o}{\partial x}$$
$$\epsilon_y^o = \frac{\partial v^o}{\partial y} \qquad (3)$$
$$\gamma_{xy}^o = \frac{\partial u^o}{\partial y} + \frac{\partial v^o}{\partial x} \quad .$$

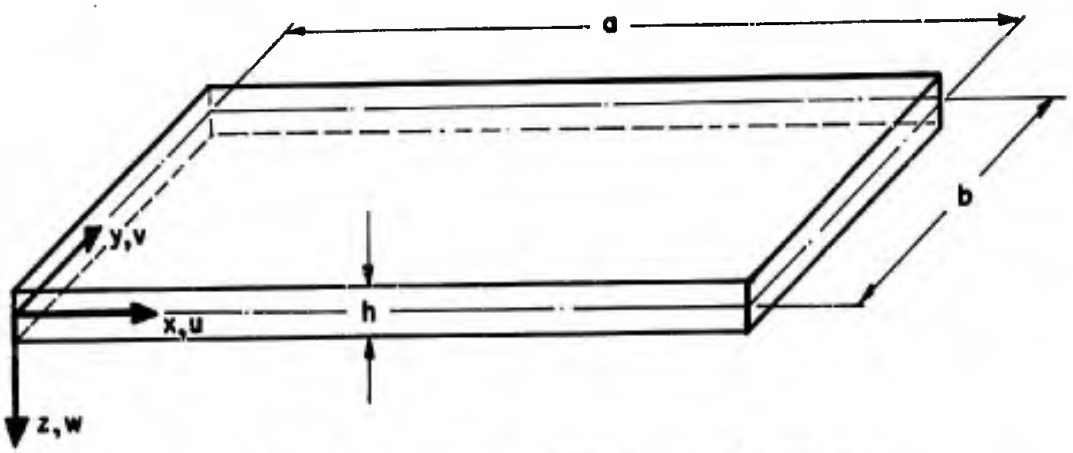

Figure 1. Plate Geometry and Displacement Directions

If normal stresses through the thickness are neglected in the comparison with σ_x and σ_y, Hooke's law yields for the stresses

$$\sigma_x = \frac{E}{1-\nu^2}\left[\epsilon_x + \nu\epsilon_y - (1+\nu)\alpha T\right]$$

$$\sigma_y = \frac{E}{1-\nu^2}\left[\epsilon_y + \nu\epsilon_x - (1+\nu)\alpha T\right] \qquad (4)$$

$$\sigma_{xy} = \sigma_{yx} = \frac{E}{2(1+\nu)}\,\gamma_{xy}$$

where $T = T(x,y,z)$ is arbitrary.

B. RESULTANT FORCES AND MOMENTS IN TERMS OF DISPLACEMENTS AND TEMPERATURES

The resultant forces and moments per unit of length

$$(N_x, N_y, N_{xy}) = \int_{-\frac{h}{2}}^{\frac{h}{2}} (\sigma_x, \sigma_y, \sigma_{xy})\,dz$$

$$(M_x, M_y, M_{xy}) = \int_{-\frac{h}{2}}^{\frac{h}{2}} (\sigma_x, \sigma_y, \sigma_{xy})\; z\; dz$$

can be expressed in terms of midplane strains and displacements by substituting Equations (2) and (4) into the above and performing the indicated integrations:

$$N_x = \frac{Eh}{1-\nu^2}\left[\epsilon_x^o + \nu\epsilon_y^o\right] - \frac{N_T}{1-\nu}$$

$$N_y = \frac{Eh}{1-\nu^2}\left[\epsilon_y^o + \nu\epsilon_x^o\right] - \frac{N_T}{1-\nu} \qquad (5a)$$

$$N_{xy} = \frac{Eh}{2(1+\nu)}\gamma_{xy}^o$$

$$M_x = -D\left[\frac{\partial^2 w}{\partial x^2} + \nu\frac{\partial^2 w}{\partial y^2}\right] - \frac{M_T}{1-\nu}$$

$$M_y = -D\left[\frac{\partial^2 w}{\partial y^2} + \nu\frac{\partial^2 w}{\partial x^2}\right] - \frac{M_T}{1-\nu} \qquad (5b)$$

$$M_{xy} = -M_{yx} = D(1-\nu)\frac{\partial^2 w}{\partial x \partial y}$$

where

$$N_T = E\int_{-\frac{h}{2}}^{\frac{h}{2}} \alpha T\, dz$$

$$M_T = E\int_{-\frac{h}{2}}^{\frac{h}{2}} \alpha T\, z\, dz \qquad (5c)$$

C. TOTAL STRESSES

From Equations (2) and (4), the total stress at any point of the plate may be expressed as

$$\sigma_x = \frac{E}{1-\nu^2}\left[\epsilon_x^o + \nu\epsilon_y^o\right] - \frac{E\alpha T}{1-\nu} - \frac{Ez}{1-\nu^2}\left[\frac{\partial^2 w}{\partial x^2} + \nu\frac{\partial^2 w}{\partial y^2}\right]$$

$$\sigma_y = \frac{E}{1-\nu^2}\left[\epsilon_y^o + \nu\epsilon_x^o\right] - \frac{E\alpha T}{1-\nu} - \frac{Ez}{1-\nu^2}\left[\frac{\partial^2 w}{\partial y^2} + \nu\frac{\partial^2 w}{\partial x^2}\right] \qquad (6a)$$

$$\sigma_{xy} = \frac{E}{2(1+\nu)}\gamma_{xy}^o - \frac{Ez}{1+\nu}\frac{\partial^2 w}{\partial x \partial y}$$

or alternately, from Equations (5) in terms of the resultant forces and moments as

$$\sigma_x = \frac{1}{h}\left(N_x + \frac{N_T}{1-\nu}\right) - \frac{E\alpha T}{1-\nu} + \frac{12z}{h^3}\left(M_x + \frac{M_T}{1-\nu}\right)$$

$$\sigma_y = \frac{1}{h}\left(N_y + \frac{N_T}{1-\nu}\right) - \frac{E\alpha T}{1-\nu} + \frac{12z}{h^3}\left(M_y + \frac{M_T}{1-\nu}\right) \qquad (6b)$$

$$\sigma_{xy} = \frac{N_{xy}}{h} - \frac{12z}{h^3} M_{xy} .$$

D. EQUILIBRIUM EQUATIONS

The three-dimensional stress equations of equilibrium in the absence of body forces are

$$\frac{\partial \sigma_x}{\partial x} + \frac{\partial \sigma_{yx}}{\partial y} + \frac{\partial \sigma_{zx}}{\partial z} = 0$$

$$\frac{\partial \sigma_{xy}}{\partial x} + \frac{\partial \sigma_y}{\partial y} + \frac{\partial \sigma_{zy}}{\partial z} = 0 \qquad (7)$$

$$\frac{\partial \sigma_{xz}}{\partial x} + \frac{\partial \sigma_{yz}}{\partial y} + \frac{\partial \sigma_z}{\partial z} = 0 .$$

Integration of the first two equations of (7) through the thickness yields

$$\frac{\partial N_x}{\partial x} + \frac{\partial N_{yx}}{\partial y} + \left[\sigma_{zx}\right]_{-\frac{h}{2}}^{\frac{h}{2}} = 0$$

$$\frac{\partial N_{xy}}{\partial x} + \frac{\partial N_y}{\partial y} + \left[\sigma_{zy}\right]_{-\frac{h}{2}}^{\frac{h}{2}} = 0 . \qquad (8a)$$

Due to the condition of zero shearing stresses at the faces of the plate, the last terms in Equations (8a) vanish, and

$$\frac{\partial N_x}{\partial x} + \frac{\partial N_{yx}}{\partial y} = 0$$

$$\frac{\partial N_{xy}}{\partial x} + \frac{\partial N_y}{\partial y} = 0 . \qquad (8b)$$

If the first two equations of (7) are first multiplied by z and then if all three are integrated through the thickness, there results

$$\frac{\partial M_x}{\partial x} - \frac{\partial M_{xy}}{\partial y} - Q_x = 0$$

$$-\frac{\partial M_{xy}}{\partial x} + \frac{\partial M_y}{\partial y} - Q_y = 0 \qquad (8c)$$

$$\frac{\partial Q_x}{\partial x} + \frac{\partial Q_y}{\partial y} - q = 0$$

where

$$Q_x = \int_{-\frac{h}{2}}^{\frac{h}{2}} \sigma_{zx}\, dz$$

$$Q_y = \int_{-\frac{h}{2}}^{\frac{h}{2}} \sigma_{zy}\, dz$$

and

$$q = \sigma_z \Big]_{-\frac{h}{2}}^{\frac{h}{2}}$$

is the resultant load intensity in the positive z direction.

E. DIFFERENTIAL EQUATIONS FOR THE IN-PLANE AND BENDING PROBLEMS

Under the assumptions of small deflection theory, the quantities N_x, N_y, N_{xy} in the in-plane equilibrium equations (8b) are independent of the deflection w, while M_x, M_y, M_{xy}, Q_x, and Q_y in Equations (8c) do not depend explicitly on u^o and v^o. Thus, the differential equations governing the in-plane and bending problems become uncoupled and may be treated independently.

For the in-plane problem, Equations (8b) are satisfied identically by the Airy stress function $\phi(x,y)$, such that

$$N_x = \frac{\partial^2 \phi}{\partial y^2}$$

$$N_y = \frac{\partial^2 \phi}{\partial x^2} \qquad (9)$$

$$N_{xy} = -\frac{\partial^2 \phi}{\partial x \partial y} \,.$$

In order to satisfy compatibility of strains in the midplane of the plate, the equation

$$\frac{\partial^2 \epsilon_x^o}{\partial y^2} + \frac{\partial^2 \epsilon_y^o}{\partial x^2} - \frac{\partial^2 \gamma_{xy}^o}{\partial x \partial y} = 0 \tag{10}$$

must be satisfied. From Equations (5a) and (9) we obtain

$$\nabla^4 \phi = -\nabla^2 N_T \tag{11}$$

where

$$\nabla^4 \equiv \nabla^2 \nabla^2 \equiv \left(\frac{\partial^2}{\partial x^2} + \frac{\partial^2}{\partial y^2} \right) \left(\frac{\partial^2}{\partial x^2} + \frac{\partial^2}{\partial y^2} \right) .$$

For the bending problem, substitution of Equations (5b) into the first two equations of (8c) yields

$$\begin{aligned} Q_x &= -\frac{\partial}{\partial x} \left[D \nabla^2 w + \frac{M_T}{1-\nu} \right] \\ Q_y &= -\frac{\partial}{\partial y} \left[D \nabla^2 w + \frac{M_T}{1-\nu} \right] . \end{aligned} \tag{12}$$

If the load intensity $q = 0$, the third equation of (8c) may then be written as

$$D \nabla^4 w + \frac{\nabla^2 M_T}{1-\nu} = 0 . \tag{13}$$

Equations (11) and (13) are, respectively, the basic differential equations governing the in-plane and bending problems.

SECTION III - SOLUTION OF THE IN-PLANE PROBLEMS

In this section, general solutions for the three in-plane problems, i.e., Cases I, II, and III, will be developed. The solutions thus obtained must satisfy Equation (11) subject to the appropriate boundary conditions, where N_T is an arbitrary function of x and y. However, instead of solving these boundary value problems directly, an alternate approach will be employed in which equivalent variational problems are solved. To accomplish this, energy type functionals will be formulated such that (out of the entire class of mathematically admissible functions which satisfy the boundary conditions) those functions which render the energy functionals stationary will also satisfy the differential equations. This implies that the Euler equations of the variational problem are the differential equations to be solved.

A. CASE I: IMMOVABLE EDGES

This condition requires that $u^o = v^o = 0$ on all edges. Solution of Equation (11) subject to these boundary conditions is cumbersome if the stress function ϕ (Equations 9)is employed. It is convenient instead to deal more directly with the displacements u^o and v^o. Substitution of Equations (5a) and (3) into (8b) gives the following in-plane displacement equilibrium equations:

$$\frac{E}{2(1-\nu)}\frac{\partial}{\partial x}\left[\frac{\partial u^o}{\partial x}+\frac{\partial v^o}{\partial y}\right]+\frac{E}{2(1+\nu)}\nabla^2 u^o-\frac{1}{h(1-\nu)}\frac{\partial N_T}{\partial x}=0$$

$$\frac{E}{2(1-\nu)}\frac{\partial}{\partial y}\left[\frac{\partial u^o}{\partial x}+\frac{\partial v^o}{\partial y}\right]+\frac{E}{2(1+\nu)}\nabla^2 v^o-\frac{1}{h(1-\nu)}\frac{\partial N_T}{\partial y}=0 \qquad (14a)$$

which must be solved subject to

$$u^o = 0$$
$$v^o = 0 \qquad (14b)$$

at the edges.

Solving this boundary value problem is equivalent to solving a plane stress problem where again the edges are immovable but the temperature does not vary through the thickness. To show this, let the displacement components in this hypothetical plane stress problem be denoted by $\bar{u}$ and $\bar{v}$, while the planform temperature (which does not vary through the thickness) is denoted by $\bar{T}$. To obtain the plane stress solution we must solve (Reference 2)

$$\frac{E}{2(1-\nu)}\frac{\partial}{\partial x}\left[\frac{\partial \bar{u}}{\partial x}+\frac{\partial \bar{v}}{\partial y}\right]+\frac{E}{2(1+\nu)}\nabla^2 \bar{u}-\frac{1}{h(1-\nu)}\frac{\partial(E\alpha \bar{T}h)}{\partial x}=0$$

$$\frac{E}{2(1-\nu)}\frac{\partial}{\partial y}\left[\frac{\partial \bar{u}}{\partial x}+\frac{\partial \bar{v}}{\partial y}\right]+\frac{E}{2(1+\nu)}\nabla^2 \bar{v}-\frac{1}{h(1-\nu)}\frac{\partial(E\alpha \bar{T}h)}{\partial y}=0 \qquad (15a)$$

subject to

$$\bar{u} = 0$$
$$\bar{v} = 0 \tag{15b}$$

at the edges.

Employing the principle of minimum potential energy, the solution of Equations (15a) may be obtained by making the strain energy

$$U = \int_0^a \int_0^b \left\{ \frac{Eh}{2(1-\nu^2)} \left[\left(\frac{\partial \bar{u}}{\partial x} \right)^2 + \left(\frac{\partial \bar{v}}{\partial y} \right)^2 + 2\nu \frac{\partial \bar{u}}{\partial x} \frac{\partial \bar{v}}{\partial y} \right. \right.$$
$$\left. - 2(1+\nu)\, \alpha\, \bar{T} \left(\frac{\partial \bar{u}}{\partial x} + \frac{\partial \bar{v}}{\partial y} \right) + \frac{1-\nu}{2} \left(\frac{\partial \bar{u}}{\partial y} + \frac{\partial \bar{v}}{\partial x} \right)^2 \right] + \left. \frac{Eh(\alpha \bar{T})^2}{1-\nu} \right\} dx\, dy \tag{16}$$

stationary subject to Equations (15b).

At this point we note that the system of Equations (14a) becomes identical to the system of Equations (15a) if in Equations (14a) u^o and v^o are replaced by $\bar{u}$ and $\bar{v}$, while $E\alpha Th$ is replaced by N_T. Thus, because of the mathematical equivalence, the solution of Equations (14a) may be obtained by making the functional

$$H = \int_0^a \int_0^b \left\{ \frac{Eh}{2(1-\nu^2)} \left[\left(\frac{\partial u^o}{\partial x} \right)^2 + \left(\frac{\partial v^o}{\partial y} \right)^2 + 2\nu \frac{\partial u^o}{\partial x} \frac{\partial v^o}{\partial y} \right. \right.$$
$$\left. - 2(1+\nu) \frac{N_T}{Eh} \left(\frac{\partial u^o}{\partial x} + \frac{\partial v^o}{\partial y} \right) + \frac{1-\nu}{2} \left(\frac{\partial u^o}{\partial y} + \frac{\partial v^o}{\partial x} \right)^2 \right] + \left. \frac{(N_T)^2}{(1-\nu)\, Eh} \right\} dx\, dy \tag{17}$$

stationary subject to Equations (14b).

Representing the displacements u^o and v^o in the form of a double Fourier series,

$$u^o = \sum_{m=1}^{\infty} \sum_{n=1}^{\infty} a_{mn} \sin \frac{m\pi x}{a} \sin \frac{n\pi y}{b}$$
$$v^o = \sum_{m=1}^{\infty} \sum_{n=1}^{\infty} b_{mn} \sin \frac{m\pi x}{a} \sin \frac{n\pi y}{b} \tag{18}$$

the boundary conditions are satisfied termwise.

Substitution of Equations (5a), (3), and (18) into Equation (17) yields an expression in terms of the displacement coefficients as follows:

$$H = \int_0^a \int_0^b \frac{Eh}{2(1-\nu^2)} \Big[\Big(\Sigma\Sigma\, a_{mn} \frac{m\pi}{a} \cos\frac{m\pi x}{a} \sin\frac{n\pi y}{b} \Big)^2$$

$$+ \Big(\Sigma\Sigma\, b_{mn} \frac{n\pi}{b} \sin\frac{m\pi x}{a} \cos\frac{n\pi y}{b}\Big)^2$$

$$+ 2\nu \Big(\Sigma\Sigma\, a_{mn} \frac{m\pi}{a} \cos\frac{m\pi x}{a} \sin\frac{n\pi y}{b} \Big) \Big(\Sigma\Sigma\, b_{mn} \frac{n\pi}{b} \sin\frac{m\pi x}{a} \cos\frac{n\pi y}{b}\Big)$$

$$+ \frac{1-\nu}{2} \Big(\Sigma\Sigma\, a_{mn} \frac{n\pi}{b} \sin\frac{m\pi x}{a} \cos\frac{n\pi y}{b} + \Sigma\Sigma\, b_{mn} \frac{m\pi}{a} \cos\frac{m\pi x}{a} \sin\frac{n\pi y}{b}\Big)^2$$

$$- \frac{2N_T}{Eh}(1+\nu)\Big(\Sigma\Sigma\, a_{mn} \frac{m\pi}{a} \cos\frac{m\pi x}{a} \sin\frac{n\pi y}{b}$$

$$+ \Sigma\Sigma\, b_{mn} \frac{n\pi}{b} \sin\frac{m\pi x}{a} \cos\frac{n\pi y}{b}\Big)$$

$$+ 2(1+\nu)\Big(\frac{N_T}{Eh}\Big)^2 \Big] \, dx\, dy.$$

According to the principle of minimum potential energy, the functional H must be stationary and must therefore satisfy the condition

$$\frac{\partial H}{\partial a_{rs}} = \frac{\partial H}{\partial b_{rs}} = 0.$$

This leads to the following infinite system of linear algebraic equations for the coefficients:

$$a_{rs}\Big[2\Big(\frac{r}{a}\Big)^2 + (1-\nu^2)\Big(\frac{s}{b}\Big)^2 \Big] \pi^2$$

$$+ \frac{4(1+\nu)\,rs}{ab} \sum_{\substack{m=1,2\ldots \\ m\neq r}}^{\infty} \sum_{\substack{n=1,2\ldots \\ n\neq s}}^{\infty} \Big[1-(-1)^{m+r}\Big]\Big[1-(-1)^{n+s}\Big] \frac{mn\, b_{mn}}{(m^2-r^2)(s^2-n^2)}$$

(19a)

$$- \frac{8(1+\nu)\,r\pi}{a^2 b} \int_0^a \int_0^b \Big(\frac{N_T}{Eh}\Big) \cos\frac{r\pi x}{a} \sin\frac{s\pi y}{b}\, dx\, dy = 0$$

$$b_{rs}\left[2\left(\frac{s}{b}\right)^2+(1-\nu)\left(\frac{r}{a}\right)^2\right]\pi^2$$

$$+\frac{4(1+\nu)\,rs}{ab}\sum_{\substack{m=1,2\ldots\\ m\neq r}}^{\infty}\sum_{\substack{n=1,2\ldots\\ n\neq s}}^{\infty}\left[1-(-1)^{m+r}\right]\left[1-(-1)^{n+s}\right]\frac{mn\,a_{mn}}{(n^2-s^2)(r^2-m^2)}$$

$$-\frac{8(1+\nu)\,s\,\pi}{ab^2}\int_0^a\int_0^b\left(\frac{N_T}{Eh}\right)\cos\frac{s\pi y}{b}\sin\frac{r\pi x}{a}\,dx\,dy=0 \qquad (19b)$$

where $r = 1,2\ldots$, $s = 1,2\ldots$.

In order to obtain numerical solutions, it is necessary to truncate this infinite system, which implies that the Fourier series given by Equations (18) are replaced by finite series of the form

$$u^o = \sum_{m=1}^{M}\sum_{n=1}^{N} a_{mn}\sin\frac{m\pi x}{a}\sin\frac{n\pi y}{b}$$

$$v^o = \sum_{m=1}^{M}\sum_{n=1}^{N} b_{mn}\sin\frac{m\pi x}{a}\sin\frac{n\pi y}{b} \qquad (20)$$

However, this can be done to any required degree of precision and thus permits an accurate numerical solution for the displacements u^o and v^o. Further discussion of this is given in Section V. Once the displacements have been obtained in this manner, the strains and stresses are readily obtained from Equations (3) and (4).

B. CASE II: EDGES UNRESTRAINED TANGENTIALLY BUT NORMALLY IMMOVABLE

As in Case I, it is convenient to deal directly with the displacements and employ an energy approach. The condition that the edges are restrained against normal displacements requires that

$$u^o = 0 \quad ; \quad x = 0,\ a$$

$$v^o = 0 \quad ; \quad y = 0,\ b \qquad (21a)$$

while free tangential motion (along the edges) implies that the shearing forces N_{xy} and consequently the midsurface shearing strains γ^o_{xy} are zero at all edges, i.e.,

$$\frac{\partial u^o}{\partial y}+\frac{\partial v^o}{\partial x}=0\,;\quad \begin{matrix}x=0,\ a\\ y=0,\ b\end{matrix} \qquad (21b)$$

The above boundary conditions are satisfied termwise if the displacements are expressed in the form

$$u^o = \sum_{m=1}^{\infty} \sum_{n=0}^{\infty} a_{mn} \sin \frac{m\pi x}{a} \cos \frac{n\pi y}{b}$$

$$v^o = \sum_{m=0}^{\infty} \sum_{n=1}^{\infty} b_{mn} \cos \frac{m\pi x}{a} \sin \frac{n\pi y}{b} \quad . \tag{22}$$

Following the procedure of Case I these displacements are substituted into the expression for total strain energy, which is then extremized (made a local minimum) with respect to the coefficients. There results

$$a_{mo} = \frac{2(1+\nu)}{bm\pi} \int_0^b \int_0^a \cos \frac{m\pi x}{a} \left(\frac{N_T}{Eh}\right) dx\, dy \quad (m = 1,2\ldots)$$

$$b_{on} = \frac{2(1+\nu)}{an\pi} \int_0^b \int_0^a \cos \frac{n\pi y}{b} \left(\frac{N_T}{Eh}\right) dx\, dy \quad (n = 1,2\ldots) \tag{23a}$$

$$a_{mn} = \frac{4(1+\nu)m\pi}{a^2 b\left[\left(\frac{m\pi}{a}\right)^2 + \left(\frac{n\pi}{b}\right)^2\right]} \int_0^b \int_0^a \cos \frac{m\pi x}{a} \cos \frac{n\pi y}{b} \left(\frac{N_T}{Eh}\right) dx\, dy$$

$$b_{mn} = \left(\frac{n}{m}\right)\left(\frac{a}{b}\right) a_{mn} \quad \begin{matrix}(m = 1,2\ldots)\\(n = 1,2\ldots)\end{matrix} . \tag{23b}$$

Thus the Fourier coefficients of Equations (22) have been determined explicitly.

C. CASE III: FREE PLATE

When the edges of the plate are unrestrained, i.e., stress free, the boundary conditions in terms of the stress function ϕ (x, y) are

$$\phi = 0 \text{ and } \frac{\partial \phi}{\partial x} = 0 ; \quad x = 0, a$$

$$\phi = 0 \text{ and } \frac{\partial \phi}{\partial y} = 0 ; \quad y = 0, b. \tag{24}$$

Thus the solution for the stresses in the plate may be obtained by first solving Equation (11) subject to the conditions of Equations (24). However, it may be shown that this problem is equivalent to extremizing the functional (Reference 3)

$$H = \int_0^a \int_0^b \left\{ \left[\nabla^2 \phi\right]^2 + 2\left[\nabla^2 N_T\right] \phi \right\} dx\, dy \tag{25}$$

subject to the same boundary constraints (Equations 24). Utilizing this approach, we construct the complete class of functions

$$\phi = x^2 (x-a)^2 y^2 (y-b)^2 \sum_{m=0}^{\infty} \sum_{n=0}^{\infty} c_{mn} x^m y^n \tag{26}$$

which automatically satisfy the conditions of Equations (24). Substituting Equation (26) into Equation (25) and imposing the stationary requirement $\frac{\partial H}{\partial c_{rs}} = 0$ results in

$$\sum_{m=0}^{\infty} \sum_{n=0}^{\infty} c_{mn} \left[(I)\ a^{r+m+5} b^{s+n+9} + 2 (II)\ a^{r+m+7} b^{s+n+7} + (III)\ a^{r+m+9} b^{s+n+5} \right] + \int_0^a \int_0^b L\, dx\, dy = 0 ; \quad \begin{matrix} (r = 1,2\ldots) \\ (s = 1,2\ldots) \end{matrix} \tag{27a}$$

where

$$(I) = \frac{576\ (r+2)(r+1)(m+2)(m+1)(m+r)!\ \ (n+s+4)!}{(m+r+5)!\ \ (n+s+9)!}$$

$$(II) = \frac{16\left[(m-6)(m+1) + (r-6)(r+1) - 4rm\right]\left[(n-6)(n+1) + (s-6)(s+1) - 4sn\right](m+r+2)!\ (n+s+2)!}{(m+r+7)!\ \ (n+s+7)!}$$

$$(III) = \frac{576\ (s+2)(s+1)(n+2)(n+1)(n+s)!\ \ (r+m+4)!}{(n+s+5)!\ \ (m+r+9)!} \tag{27b}$$

and

$$L = (x^{r+4} - 2ax^{r+3} + a^2 x^{r+2})\ (y^{s+4} - 2by^{s+3} + b^2 y^{s+2})\ \nabla^2\ N_T .$$

Equations (27) comprise an infinite system of linear algebraic equations in the unknowns c_{mn} which cannot be solved exactly. Accurate numerical results can be obtained, however, by an appropriate truncation of the representation of ϕ (Equation (26)) as described in Section V.

SECTION IV - SOLUTION OF THE BENDING PROBLEMS

Solutions of the bending problems, Cases IV and V, for clamped and simply supported plates subject to arbitrary three-dimensional temperature distributions are given in this section.

A. CASE IV: CLAMPED PLATE

The boundary conditions are:

$$w = 0 \text{ and } \frac{\partial w}{\partial x} = 0 \quad ; \quad x = 0, a$$

$$w = 0 \text{ and } \frac{\partial w}{\partial y} = 0 \quad ; \quad y = 0, b \ . \tag{28}$$

A comparison of the system of Equations (13) and (28) with that of Equations (11) and (24) reveals that the solution of the clamped bending problem is mathematically equivalent to the solution of the free in-plane problem if, in the latter case, ϕ is replaced by w and N_T by $M_T/D(1-\nu)$. With this interchange, the solution is thus given by Equation (26) which becomes

$$w = x^2 (x-a)^2 y^2 (y-b)^2 \sum_{m=0}^{\infty} \sum_{n=0}^{\infty} C_{mn} x^m y^n \ . \tag{29}$$

The coefficients in Equation (29) are obtained from Equations (27) where

$$L = (x^{r+4} - 2a\, x^{r+3} + a^2 x^{r+2})(y^{s+4} - 2by^{s+3} + b^2 y^{s+2}) \frac{\nabla^2 M_T}{D(1-\nu)} \ . \tag{30}$$

B. CASE V: SIMPLY SUPPORTED PLATE

Here the deflections and bending moments are zero on all edges, which implies

$$w = 0$$

$$\nabla^2 w + \frac{M_T}{D(1-\nu)} = 0 \tag{31}$$

on all edges. If we define $\nabla^2 w = P$, then Equation (13) becomes

$$\nabla^2 \left[P + \frac{M_T}{D(1-\nu)} \right] = 0 \tag{32}$$

where, from Equations (31)

$$P + \frac{M_T}{D(1-\nu)} = 0 \tag{33}$$

on all edges. Then, from the maximum and minimum value theorem for harmonic functions (Reference 4)

$$P + \frac{M_T}{D(1-\nu)} \equiv 0 \; ; \qquad \begin{matrix} 0 \le x \le a \\ 0 \le y \le b \, . \end{matrix} \tag{34}$$

Therefore, the problem reduces to solving

$$\nabla^2 w = - \frac{M_T}{D(1-\nu)} \tag{35}$$

subject to

$$w = 0 \tag{36}$$

on all edges. By using the Fourier series representation

$$\frac{M_T}{D(1-\nu)} = \sum_{m=1}^{\infty} \sum_{n=1}^{\infty} a_{mn} \sin \frac{m\pi x}{a} \sin \frac{n\pi y}{b} \tag{37}$$

where a_{mn} are the usual Fourier coefficients, it is readily verified that

$$w = \sum_{m=1}^{\infty} \sum_{n=1}^{\infty} \frac{a_{mn}}{\left(\frac{m\pi}{a}\right)^2 + \left(\frac{n\pi}{b}\right)^2} \sin \frac{m\pi x}{a} \sin \frac{n\pi y}{b} \, . \tag{38}$$

The moments in the plate can be obtained by substituting Equation (38) into Equations (5b). At the edges, however, the resultant Fourier series expressions for the bending moments are invalid. To remedy this situation, the computer program imposes the constraint conditions

$$\left.\begin{matrix} M_x = 0 \\ M_y = - M_T \end{matrix}\right\} \qquad \left\{\begin{matrix} \xi = 0, \, 1 \\ 0 < \eta < 1 \end{matrix}\right\}$$

and

$$\left.\begin{matrix} M_y = 0 \\ M_x = - M_T \end{matrix}\right\} \qquad \left\{\begin{matrix} 0 < \xi < 1 \\ \eta = 0, \, 1 \end{matrix}\right\} \, .$$

Everywhere in the plate interior, the Fourier series for the bending moments yield the correct solutions, although near the edges convergence is slow.

SECTION V - DESCRIPTION OF COMPUTER PROGRAM

The complete program for the determination of stresses and deflections due to three-dimensional heating is subdivided into two major phases:

(1) Heat Transfer Program for the determination of time dependent (transient) temperatures.

(2) Stress Analysis Program for the evaluation of the quasi-static stresses and deflections.

The integration of these two phases permits the continuous flow from given heat input, material, and geometry data to the deflection and stress responses. Detailed descriptions of the program formulations are given below.

A. HEAT TRANSFER PROGRAM*

1. GENERAL DESCRIPTION

The solution of the heat transfer problem is based upon the Fourier heat conduction equation in rectangular coordinates

$$\rho\, c \frac{\partial T}{\partial t} = K \nabla^2 T \tag{39}$$

where

$$\nabla^2 = \frac{\partial^2}{\partial x^2} + \frac{\partial^2}{\partial y^2} + \frac{\partial^2}{\partial z^2}$$

and

ρ = density
c = specific heat
K = thermal conductivity.

Note that in Equation (39) space gradients of K have been neglected. Aside from this approximation, K, ρ, and c are permitted to be temperature dependent. They thus vary with the spatial coordinates and time.

For the rectangular plate, two types of boundary conditions are accommodated by the program.

Type 1: Temperature is given on a bounding surface as a function of time and position.

Type 2: A heat flux condition is specified, of the form

$$\frac{K \partial T}{\partial n} = H (T - T_w) + \epsilon \sigma (T^4 - T_w^4) - S \tag{40}$$

where

n = inward surface normal
H = surface heat transfer coefficient
ϵ = emissivity
σ = Stefan-Boltzmann's constant

* This subsection is due principally to the efforts of M. Gershinsky.

T_w = adiabatic wall temperature

S = heat flux to surface .

For transient problems, the initial temperature must be given in addition to the boundary conditions.

2. NUMERICAL ANALYSIS

Numerical solutions are obtained by imposing a rectangular mesh on the plate, with the understanding that the finer the mesh, the closer is the approximation to the exact problem. For each mesh point, a finite difference equivalent of Equation (39) is written. $T_{i,j,k,n}$ denotes the temperature at the i^{th} point in the x direction, the j^{th} point in the y direction, the k^{th} point in the z direction, and the n^{th} time step (the n subscript is omitted for steady-state problems). The expression $\rho c \frac{\partial T}{\partial t}$ is then approximated by a central difference expression at mid-time $t + \frac{\Delta t}{2}$ as

$$\rho c \frac{T_{i,j,k,n+1} - T_{i,j,k,n}}{\Delta t}$$

where c is determined by the time average of temperature at the point. The right-hand side of Equation (39) is also evaluated at mid-time as the average of the central difference operators at times t and $t + \Delta t$. Therefore

$$K\nabla^2 T \sim \frac{K_{t+(\Delta t/2)}}{2(\Delta x)^2}\left[\left(T_{i+1,j,k,n} - 2T_{i,j,k,n} + T_{i-1,j,k,n}\right) + \left(T_{i+1,j,k,n+1} - 2T_{i,j,k,n+1} + T_{i-1,j,k,n+1}\right)\right] + \ldots$$

When the approximations to $\rho c \frac{\partial T}{\partial t}$ and $K\nabla^2 T$ are equated, a system of algebraic equations is obtained. These, together with the boundary conditions, are solved for $T_{i,j,k,n+1}$ in terms of all the other T terms by a Gauss-Seidel type iteration procedure.

3. INPUT TO THE PROGRAM

The following input data are required by the program:

(1) a, b, h (plate dimensions)
(2) H (surface heat transfer coefficient) as a function of both temperature and time
(3) T_w (adiabatic wall temperature) as a function of time for each boundary
(4) S (heat flux to surface) in the form of a product of functions of time, position, and temperature
(5) K (thermal conductivity)
(6) c (specific heat)
(7) ϵ (emissivity)

where items (5) - (7) are given as functions of temperature in tabular form.

The initial temperature distribution is to be determined by means of linear interpolation in the z direction of the initial temperatures at the faces $z = \pm \frac{h}{2}$. If the boundary conditions are given as prescribed temperatures on the faces $z = \pm \frac{h}{2}$, they may be represented in the form

$$\left[f_1 (x, y) \right] \left[f_2 (t) \right] + f_3 (t).$$

The program is such that, on the edges, the temperature or flux boundary conditions must be given as functions of time alone.

The time intervals may be specified arbitrarily. However, upon failure to converge, they will automatically be reduced by half.

Temperature or flux boundary data on the faces $z = \pm \frac{h}{2}$ are to be specified in sets of discrete nine-point arrays (clusters) as shown in Figure 2. Within each cluster the data are matched exactly at the nine points by a polynomial of the form

$\sum_{m=0}^{2} \sum_{n=0}^{2} a_{mn} x^m y^n$. This yields approximating analytic representations of the temperature or flux conditions over the bounding faces.

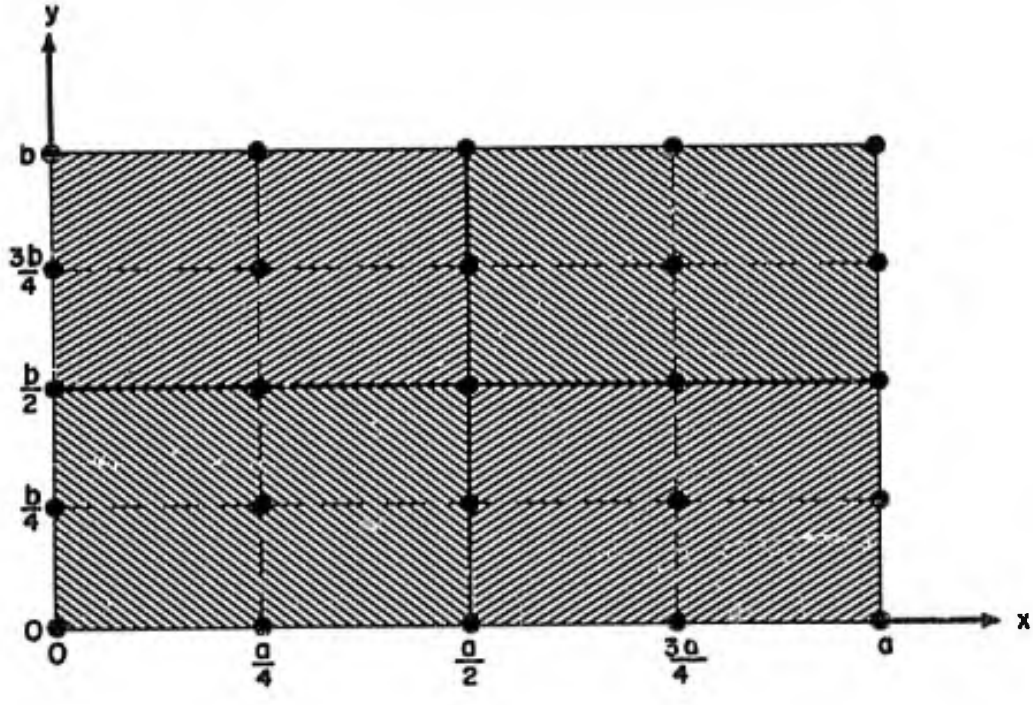

Figure 2. Plate Planform Subdivided into Four Nine-Point Clusters

4. PROGRAM LOGIC

The transient problem determines the temperatures at time $t + \Delta t$, given the temperatures at time t and employing the numerical equations. As the first estimate of temperatures at time $t + \Delta t$, the program uses the temperatures at time t. A relative test is employed to determine whether the most recent approximation indicates convergence, and the solution is accepted only if convergence takes place at all points. If the iteration process fails to converge within a specified maximum number of iterations, the time interval is reduced by half. If the number of cutbacks exceeds a specified maximum in any one time interval, a failure to converge is acknowledged.

The steady-state problem can be solved in two ways:

(1) By direct solution based on the boundary conditions.

(2) By solving the transient problem up to any time t and then using this transient solution as a first approximation to the steady-state solution.

B. STRESS ANALYSIS PROGRAM

1. NONDIMENSIONAL COMPUTATIONAL FORMULAS

In order to standardize the numerical procedures for computing purposes, the five solutions presented in Sections III and IV were nondimensionalized by defining the quantities:

$$\bar{N}_x = \frac{b(1-\nu)}{Eh^2} N_x$$

$$\bar{N}_y = \frac{b(1-\nu)}{Eh^2} N_y \qquad (41)$$

$$\bar{N}_{xy} = \frac{2b(1+\nu)}{Eh^2} N_{xy}$$

$$\bar{w} = \frac{w}{h}$$

$$\bar{M}_x = \frac{b^2}{Dh} M_x$$

$$\bar{M}_y = \frac{b^2}{Dh} M_y \qquad (42)$$

$$\bar{M}_{xy} = \frac{b^2}{Dh} M_{xy}$$

$$\bar{N}_T = \frac{b}{Eh^2} N_T; \quad \bar{M}_T = \frac{b^2}{(1-\nu)Dh} M_T \qquad (43)$$

$$\lambda = \frac{a}{b}, \; \xi = \frac{x}{a}, \; \eta = \frac{y}{b}.$$

In terms of the above nondimensional quantities, the problem solutions reduce to the following forms:

a. In-Plane Problems

Case I

$$\bar{N}_x = \frac{1}{1+\nu} \sum_{m=1}^{\infty} \sum_{n=1}^{\infty} \left[\frac{m\pi}{\lambda} A_{mn} \cos m\pi\xi \sin n\pi\eta + \nu n\pi B_{mn} \sin m\pi\xi \cos n\pi\eta \right] - \bar{N}_T$$

$$\bar{N}_y = \frac{1}{1+\nu} \sum_{m=1}^{\infty} \sum_{n=1}^{\infty} \left[n\pi B_{mn} \sin m\pi\xi \cos n\pi\eta + \frac{\nu}{\lambda} m\pi A_{mn} \cos m\pi\xi \sin n\pi\eta \right] - \bar{N}_T \qquad (44)$$

$$\bar{N}_{xy} = \sum_{m=1}^{\infty} \sum_{n=1}^{\infty} \left[n\pi A_{mn} \sin m\pi\xi \cos n\pi\eta + \frac{m\pi}{\lambda} B_{mn} \cos m\pi\xi \sin n\pi\eta \right]$$

where the coefficients A_{mn} and B_{mn} are determined from

$$A_{rs}\left[\frac{2r^2}{\lambda} + (1-\nu)\lambda s^2 \right] \pi^2 + 4(1+\nu) rs \sum_{\substack{m=1 \\ m\neq r}}^{\infty} \sum_{\substack{n=1 \\ n\neq s}}^{\infty} \left[1 - (-1)^{m+r} \right] \left[1 - (-1)^{n+s} \right] \frac{mn\, B_{mn}}{(m^2-r^2)(s^2-n^2)}$$

$$= 8(1+\nu) r\pi \int_0^1 \int_0^1 \bar{N}_T \cos r\pi\xi \sin s\pi\eta \, d\xi \, d\eta \qquad (45)$$

$$B_{rs}\left[2\lambda s^2 + (1-\nu)\frac{r^2}{\lambda} \right] \pi^2 + 4(1+\nu) rs \sum_{\substack{m=1 \\ m\neq r}}^{\infty} \sum_{\substack{n=1 \\ n\neq s}}^{\infty} \left[1 - (-1)^{m+r} \right] \left[1 - (-1)^{n+s} \right] \frac{mn\, A_{mn}}{(n^2-s^2)(r^2-m^2)}$$

$$= 8(1+\nu)(s\pi\lambda) \int_0^1 \int_0^1 \bar{N}_T \cos s\pi\eta \sin r\pi\xi \, d\xi \, d\eta$$

Case II

$$\bar{N}_x = \frac{\pi}{1+\nu}\left[\frac{1}{\lambda}\sum_{m=1}^{\infty}\sum_{n=0}^{\infty} m\, a_{mn} \cos m\pi\xi \cos n\pi\eta + \nu\sum_{m=0}^{\infty}\sum_{n=1}^{\infty} n\, b_{mn} \cos m\pi\xi \cos n\pi\eta\right] - \bar{N}_T$$

$$\bar{N}_y = \frac{\pi}{1+\nu}\left[\sum_{m=0}^{\infty}\sum_{n=1}^{\infty} n\, b_{mn} \cos m\pi\xi \cos n\pi\eta + \frac{\nu}{\lambda}\sum_{m=1}^{\infty}\sum_{n=0}^{\infty} m\, a_{mn} \cos m\pi\xi \cos n\pi\eta\right] - \bar{N}_T \qquad (46)$$

$$\bar{N}_{xy} = -\pi\sum_{m=1}^{\infty}\sum_{n=0}^{\infty}\left(n\, a_{mn} + \frac{m}{\lambda}\, b_{mn}\right) \sin m\pi\xi \sin n\pi\eta$$

where

$$a_{mo} = \frac{2(1+\nu)\lambda}{m\pi}\int_0^1\int_0^1 \cos m\pi\xi\, \bar{N}_T\, d\xi\, d\eta \qquad (m = 1, 2, \ldots.)$$

$$b_{on} = \frac{2(1+\nu)}{n\pi}\int_0^1\int_0^1 \cos n\pi\eta\, \bar{N}_T\, d\xi\, d\eta \qquad (n = 1, 2, \ldots) \qquad (47)$$

$$a_{mn} = \frac{4(1+\nu)}{\pi\left[\frac{m}{\lambda} + \frac{n^2\lambda}{m}\right]}\int_0^1\int_0^1 \cos m\pi\xi \cos n\pi\eta\, \bar{N}_T\, d\xi\, d\eta \qquad (m = 1, 2, \ldots. \; n = 1, 2, \ldots.)$$

$$b_{mn} = \frac{n}{m}\lambda\, a_{mn} \qquad (m = 1, 2, \ldots. \; n = 1, 2, \ldots.) \qquad (48)$$

Case III

$$\bar{N}_x = (1-\nu)\left[\xi(\xi-1)\right]^2\sum_{m=0}^{\infty}\sum_{n=0}^{\infty} B_{mn}\, \xi^m \eta^n\left[(n+4)(n+3)\eta^2 - 2(n+3)(n+2)\eta + (n+2)(n+1)\right] \qquad (49)$$

$$\bar{N}_y = \frac{1-\nu}{\lambda^2}\left[\eta(\eta-1)\right]^2 \sum_{m=0}^{\infty}\sum_{n=0}^{\infty} B_{mn}\,\xi^m\,\eta^n\left[(m+4)(m+3)\,\xi^2 - 2(m+3)(m+2)\,\xi + (m+2)(m+1)\right]$$

(49 cont'd)

$$\bar{N}_{xy} = \frac{-2(1+\nu)}{\lambda}\,\xi\,\eta \sum_{m=0}^{\infty}\sum_{n=0}^{\infty} B_{mn}\,\xi^m\,\eta^n\left[(m+4)\,\xi^2 - 2(m+3)\,\xi + (m+2)\right]\cdot \left[(n+4)\,\eta^2 - 2(n+3)\,\eta + (n+2)\right]$$

where the coefficients B_{mn} are determined from

$$\sum_{m=0}^{\infty}\sum_{n=0}^{\infty} B_{mn}\left[\frac{\text{(I)}}{\lambda^2} + 2\,\text{(II)} + \lambda^2\,\text{(III)}\right]$$

$$+\int_0^1\int_0^1\Big[\eta^2(\eta-1)^2\left\{(r+4)(r+3)\,\xi^2 - 2(r+3)(r+2)\,\xi + (r+2)(r+1)\right\} \qquad (50)$$

$$+\lambda^2\xi^2(\xi-1)^2\left\{(s+4)(s+3)\,\eta^2 - 2(s+3)(s+2)\,\eta + (s+2)(s+1)\right\}\Big]\,\xi^r\,\eta^s\,\bar{N}_T\,d\xi\,d\eta = 0$$

and quantities (I), (II), and (III) are given by Equation (27b).

b. Bending Problems

Case IV

$$\bar{w} = \left[\xi(\xi-1)(\eta)(\eta-1)\right]^2 \sum_{m=0}^{\infty}\sum_{n=0}^{\infty} B_{mn}\,\xi^m\,\eta^n \qquad (51)$$

$$\bar{M}_x = -\left(\frac{1}{\lambda^2}\frac{\partial^2\bar{w}}{\partial\xi^2} + \nu\frac{\partial^2\bar{w}}{\partial\eta^2} + \bar{M}_T\right)$$

$$\bar{M}_y = -\left(\frac{\partial^2\bar{w}}{\partial\eta^2} + \frac{\nu}{\lambda^2}\frac{\partial^2\bar{w}}{\partial\xi^2} + \bar{M}_T\right) \qquad (52)$$

$$\bar{M}_{xy} = \frac{1-\nu}{\lambda}\frac{\partial^2\bar{w}}{\partial\xi\,\partial\eta}$$

where

$$\sum_{m=0}^{\infty}\sum_{n=0}^{\infty} B_{mn}\left[\frac{\text{(I)}}{\lambda^2} + 2\,\text{(II)} + \lambda^2\,\text{(III)}\right]$$

$$+\int_0^1\int_0^1\Big[\eta^2(\eta-1)^2\left\{(r+4)(r+3)\,\xi^2 - 2(r+3)(r+2)\,\xi + (r+2)(r+1)\right\} \qquad (53)$$

$$+\lambda^2\xi^2(\xi-1)^2\left\{(s+4)(s+3)\,\eta^2 - 2(s+3)(s+2)\,\eta + (s+2)(s+1)\right\}\Big]\,\xi^r\,\eta^s\,\bar{M}_T\,d\xi\,d\eta = 0$$

and quantities (I), (II), and (III) are defined by Equations (27b).

Case V

$$\bar{w} = \frac{1}{\pi^2} \sum_{m=1}^{\infty} \sum_{n=1}^{\infty} \frac{A_{mn}}{\frac{m^2}{\lambda^2} + n^2} \sin m\pi\xi \sin n\pi\eta \tag{54}$$

$$\left.\begin{aligned}
\bar{M}_x &= \sum_{m=1}^{\infty} \sum_{n=1}^{\infty} \frac{(m^2/\lambda^2) + \nu n^2}{(m^2/\lambda^2) + n^2} A_{mn} \sin m\pi\xi \sin n\pi\eta - \bar{M}_T; \; 0 < \xi < 1, \; 0 \le \eta \le 1 \\
\bar{M}_x &= 0 \\
\bar{M}_y &= -(1-\nu)\bar{M}_T \begin{cases} \xi = 0, 1 \\ 0 < \eta < 1 \end{cases} \\
\bar{M}_y &= \sum_{m=1}^{\infty} \sum_{n=1}^{\infty} \frac{(\nu m^2/\lambda^2) + n^2}{(m^2/\lambda^2) + n^2} A_{mn} \sin m\pi\xi \sin n\pi\eta - \bar{M}_T; \; 0 \le \xi \le 1, \; 0 < \eta < 1 \\
\bar{M}_y &= 0 \\
\bar{M}_x &= -(1-\nu)\bar{M}_T \begin{cases} 0 < \xi < 1 \\ \eta = 0, 1 \end{cases} \\
\bar{M}_{xy} &= \frac{1-\nu}{\lambda} \sum_{m=1}^{\infty} \sum_{n=1}^{\infty} \frac{mn}{(m^2/\lambda^2) + n^2} A_{mn} \cos m\pi\xi \cos n\pi\eta
\end{aligned}\right\} \tag{55}$$

where

$$A_{mn} = 4 \int_0^1 \int_0^1 \bar{M}_T \sin m\pi\xi \sin n\pi\eta \, d\xi \, d\eta \tag{56}$$

2. NUMERICAL ANALYSIS

The five previous cases can be divided into three classes for purposes of numerical and programming analysis:

(1) Case I
(2) Cases III and IV
(3) Cases II and V.

Item (1) presents an infinite system of equations in coupled sets of coefficients A_{mn} and B_{mn} (Equations 45). The system must be truncated by specifying an appropriate upper limit on m and n. If, for example, m and n (and hence r and s) are permitted to take on all the values from 1 to 10, the solution vector consists of 200 elements. This involves $(200)^2$ elements in the coefficient matrix, which creates a storage problem, because the core memory of the IBM 7090 is exceeded. Analysis performed upon the problem has reduced the size of the matrix to 4 sets of submatrices, each having approximately one-eighth the size of the original matrix, thereby making possible the use of direct methods of solution.

The second class of problems, Item (2), involves an infinite system of equations for coefficients B_{mn} (Equations 50 and 53). Again, these equations must be truncated by prescribing an appropriate limit on m and n (and therefore r and s). For example, we have a set of 121 equations to solve if m and n assume all integral values from 0 to 10. However, by interchanging m and n with r and s, respectively, it becomes evident that the coefficient matrix is symmetric. We take advantage of this symmetry to reduce the storage requirements. For purposes of solution, the Cholesky method (Reference 5) is employed. This is

a direct elimination scheme preserving storage in a symmetric fashion. Numerical calculations and test cases have shown the method to be efficient; round-off errors have not distorted the results and, in practice, m and n need not be as large as 10 in order to achieve accurate solutions.

In the third class of problems, Item (3), the indicated Fourier coefficients (Equations 47, 48, and 56) are calculated explicitly by integration. Force resultants, deflections, and moments are then determined from the Fourier series (46, 54, and 55) respectively, using appropriate convergence criteria.

3. INPUT AND PROGRAM LOGIC

The following data are required as basic input into the thermal stress program:

(1) λ (aspect ratio)
(2) h (thickness)
(3) b (plate dimension in the y direction)
(4) E (Young's modulus)
(5) ν (Poisson's ratio)
(6) α (coefficient of linear thermal expansion)
(7) Temperature distribution.

The temperature distribution may be determined from the heat transfer program as a prior link in the programming chain or may be provided by some other source, such as input on cards. The temperature data must be prescribed at discrete mesh points as shown in Figure 3. Any arbitrary number of equally spaced points through the thickness are permitted. The number of mesh spaces in the ξ and η directions must be equal and even (thus automatically forming planform clusters of the type indicated in Figure 2).

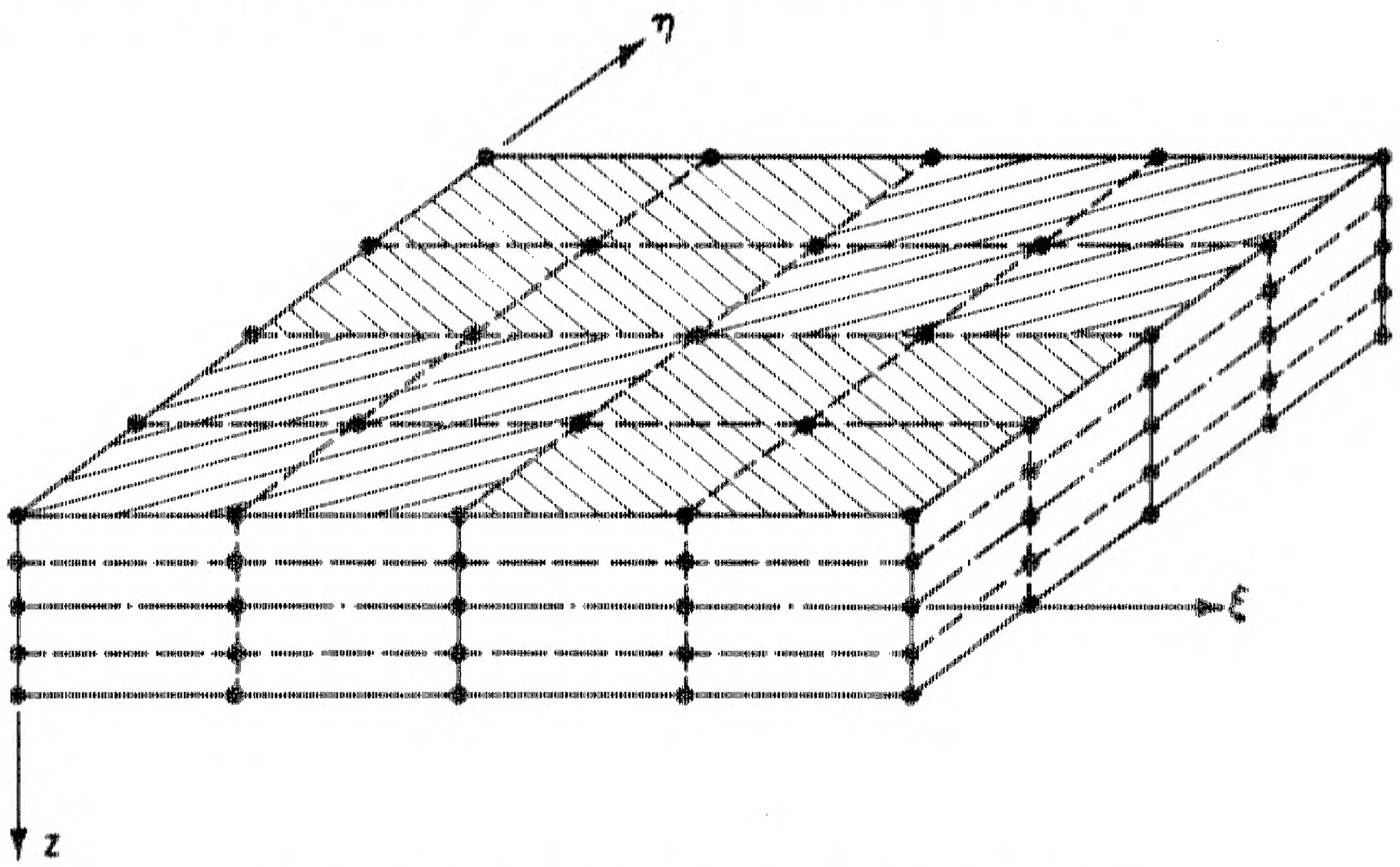

Figure 3. Typical Temperature Data Mesh Point Array

The program calculates nondimensional force resultants (Cases I, II, or III); deflections, bending moments, and twisting moments (Classes IV or V). After calculating these quantities, each according to the selected combination of cases, the results are superposed to yield the stresses and deflections at the grid points in accordance with the formulas:

$$\sigma_x = \frac{E}{1-\nu}\left[\frac{h}{b}\left(\bar{N}_x + \bar{N}_T\right) + \frac{h\,z}{b^2(1+\nu)}\left(\bar{M}_x + \bar{M}_T\right) - \alpha T\right]$$

$$\sigma_y = \frac{E}{1-\nu}\left[\frac{h}{b}\left(\bar{N}_y + \bar{N}_T\right) + \frac{h\,z}{b^2(1+\nu)}\left(\bar{M}_y + \bar{M}_T\right) - \alpha T\right] \qquad (57)$$

$$\sigma_{xy} = \frac{E\,h}{2b(1+\nu)}\left[\bar{N}_{xy} - \frac{2z}{b(1-\nu)}\bar{M}_{xy}\right]$$

$$w = \bar{w}\,h. \qquad (58)$$

The evaluation of stresses and deflections is not necessarily restricted to the mesh points at which the temperature data are specified. The program will automatically interpolate the solution to specified intermediate mesh points by means of a polynomial fit.

SECTION VI - TEST CASES SUBSTANTIATING THE VALIDITY OF THE STRESS ANALYSIS PROGRAM

In order to demonstrate the validity and accuracy of the stress analysis program, test problems were devised for each of the Cases I through V. In these problems, the forms of the temperature distributions were chosen so that accurate numerical results could be obtained by methods other than those of the present computer program. In each case, comparisons were then made between the two sets of results. The construction of the test problems and the numerical comparisons are given below for Cases II - V, where the accuracy of the numerical calculations is amply established. In Case I (immovable edges) a test problem was also devised as shown in Section VI-A. However, the computer calculations for this case revealed that more terms of the series given by Equations (44) were required for adequate convergence than had been anticipated. As a result, the core storage capacity of the IBM 7090 would be exceeded (primarily because of the additional storage requirements of Cases II - V). Thus, at present only 144 terms of the series can be accommodated, while in general several hundred terms may be needed for adequate convergence. (Nevertheless, the test problem calculations for this number of terms, although not shown in this report, did converge satisfactorily at many points of the plate.) Time limitations do not presently permit the required program modification for additional storage space. It is anticipated, however, that this will be accomplished in the near future through the use of magnetic tapes.

A. CASE I: IMMOVABLE EDGES

To date numerical results for this case have not appeared in the literature. However, closed-form analytical solutions, corresponding to a particular class of temperature functions $N_T(x, y)$, can be constructed as follows:

We seek displacement functions $u^o(x, y)$ and $v^o(x, y)$ which satisfy the boundary conditions of Equations (14b) and, when substituted into Equations (14a), yield a unique temperature function $N_T = N'_T(x, y)$. When this is accomplished, the u^o and v^o thus chosen constitute an exact solution of the displacement equations of equilibrium corresponding to N'_T. Differentiating the first and second of Equations (14a) with respect to y and x respectively and subtracting, we find that N_T is single-valued only if

$$\nabla^2 \left(\frac{\partial u^o}{\partial y} - \frac{\partial v^o}{\partial x} \right) = 0 \quad . \tag{59}$$

This requirement is certainly satisfied if we set

$$\frac{\partial u^o}{\partial y} = \frac{\partial v^o}{\partial x} \quad . \tag{60}$$

We further restrict our solution to displacement functions of the form

$$u^o = X_1(x) \cdot Y_1(y)$$
$$v^o = X_2(x) \cdot Y_2(y) \quad . \tag{61}$$

The boundary conditions of Equations (14b) require that

$$X_n(0) = X_n(a) = Y_n(0) = Y_n(b) = 0 \qquad (n = 1, 2) \quad . \tag{62}$$

Equations (60) - (62) possess many solutions. A simple solution may be obtained by selecting

$$X_2 = x^2(x - a)^2$$
$$Y_1 = y^2(y - b)^2 \quad . \tag{63}$$

From Equation (60) we then find that

$$X_1 = 2cx(x - a)(2x - a)$$
$$Y_2 = 2cy(y - b)(2y - b) \tag{64}$$

where c is an arbitrary constant. Therefore, and v^o are given by

$$u^o = cx(x - a)(2x - a)(y^2)(y - b)^2$$
$$v^o = cy(y - b)(2y - b)(x^2)(x - a)^2 \quad . \tag{65}$$

Substitution of Equations (65) into Equations (14a) yields

$$N_T = \frac{Ec\mu}{1+\nu}\left\{x^2(x-a)^2\left[6y(y-b) + b^2\right] + y^2(y-b)^2\left[6x(x-a) + a^2\right]\right\} \quad . \tag{66}$$

Inserting Equations (65) and (66) into Equations (3), (5a), (41), and (43) yields the following dimensionless stress resultants:

$$\bar{N}_x = -(1 - \nu)\,\xi^2(\xi - 1)^2(6\eta^2 - 6\eta + 1)$$
$$\bar{N}_y = -\frac{(1 - \nu)}{\lambda^2}(6\xi^2 - 6\xi + 1)\,\eta^2(\eta - 1)^2 \tag{67}$$
$$\bar{N}_{xy} = \frac{4(1 + \nu)}{\lambda}(\xi)(\xi - 1)(2\xi - 1)(\eta)(\eta - 1)(2\eta - 1)$$

where, for convenience, we have chosen

$$c = \frac{(1 + \nu)h}{a^4 b^3} \quad . \tag{68}$$

The corresponding nondimensional form of Equation (66) is

$$\bar{\bar{N}}_T = \xi^2(1-\xi)^2(6\eta^2 - 6\eta + 1) + \frac{1}{\lambda^2}\,\eta^2(1-\eta)^2(6\xi^2 - 6\xi + 1) \quad . \tag{69}$$

Thus the dimensionless stress resultants given by Equations (67) are the exact solution corresponding to the temperature distributions defined by Equation (69).

B. CASE II: EDGES UNRESTRAINED TANGENTIALLY BUT NORMALLY IMMOVABLE (FREELY SLIDING EDGES)

As in Case I, previous numerical results are not available; therefore, the accuracy of the digital computer program has been tested against a closed-form analytical solution. This solution, developed along similar lines as in Section VI-A, is now outlined.

Displacement functions u^o and v^o which satisfy the boundary conditions of Equations (21) and Equation (59) are

$$\begin{aligned} u^o &= \frac{x}{a}(a - x) \\ v^o &= \frac{y}{b}(b - y) \quad . \end{aligned} \tag{70}$$

Substituting the values of Equations (70) into Equations (14a) yields expressions which may be solved for the temperature function $N_T(x, y)$. The stress resultants may be obtained by inserting u^o, v^o, and N_T into Equations (3) and (5a). In nondimensional form, the results are given by

$$\begin{aligned} \bar{\bar{N}}_T &= \xi + \eta \\ \bar{\bar{N}}_x &= -\left[\frac{1+\nu}{2} + (1-\nu)\,\eta\right] \\ \bar{\bar{N}}_y &= -\left[\frac{1+\nu}{2} + (1-\nu)\,\xi\right] \\ \bar{\bar{N}}_{xy} &= 0 \end{aligned} \tag{71}$$

In Table I, the series solutions for $\bar{\bar{N}}_x$ and $\bar{\bar{N}}_y$ from Equations (46) that were used in the computational program are compared with the exact results of Equations (71). The data are generated for $\nu = 0.30$ and $\lambda = 1.5$. The series are evaluated for 110, 420, and 930 terms. Here, as in all the ensuing test cases, the temperature data are specified at 49 equally spaced mesh points; i.e., the planform is divided into 9 equally sized clusters.

The results show that the series approximations converge rapidly to the exact values. Thus we note from Table I that with only 110 terms the maximum error in both $\bar{\bar{N}}_x$ and $\bar{\bar{N}}_y$ occurs at $\xi = \eta = 0$ (i.e., at a corner) and has a magnitude of approximately 4%.

TABLE I

CASE II: COMPARISON OF COMPUTER CALCULATIONS WITH EXACT SOLUTION

η \ ξ	0	1/3	1/2	2/3	1	Number of Terms in Series (46)
			$\bar{N}_x$			
0	-.6237	-.6421	-.6439	-.6458	-.6641	110
	-.6368	-.6475	-.6470	-.6464	-.6571	420
	-.6412	-.6480	-.6480	-.6500	-.6547	930
	-.6500	-.6500	-.6500	-.6500	-.6500	Exact Solution
1/2	-.9793	-.9982	-1.0000	-1.0018	-1.0202	110
	-.9899	-1.0005	-1.0000	-.9995	-1.0101	420
	-.9933	-1.0000	-1.0000	-1.0000	-1.0067	930
	-1.0000	-1.0000	-1.0000	-1.0000	-1.0000	Exact Solution
1	-1.3359	-1.3542	-1.3561	-1.3579	-1.3762	110
	-1.3429	-1.3536	-1.3530	-1.3525	-1.3631	420
	-1.3453	-1.3520	-1.3520	-1.3520	-1.3588	930
	-1.3500	-1.3500	-1.3500	-1.3500	-1.3500	Exact Solution
			$\bar{N}_y$			
0	-.6237	-.8626	-.9798	-1.0970	-1.3359	110
	-.6368	-.8734	-.9899	-1.1064	-1.3429	420
	-.6412	-.8766	-.9933	-1.1099	-1.3453	930
	-.6500	-.8833	-1.0000	-1.1167	-1.3500	Exact Solution
1/2	-.6439	-.8828	-1.0000	-1.1172	-1.3561	110
	-.6470	-.8835	-1.0000	-1.1165	-1.3530	420
	-.6480	-.8833	-1.0000	-1.1167	-1.3520	930
	-.6500	-.8833	-1.0000	-1.1167	-1.3500	Exact Solution
1	-.6641	-.9030	-1.0202	-1.1374	-1.3762	110
	-.6571	-.8936	-1.0101	-1.1266	-1.3631	420
	-.6547	-.8901	-1.0068	-1.1234	-1.3588	930
	-.6500	-.8833	-1.0000	-1.1167	-1.3500	Exact Solution

C. CASE III: FREE PLATE

The force resultant N_x in a free plate when subjected to temperature distributions which satisfy

$$\nabla^2 N_T = \text{constant} \tag{72}$$

may be determined from the approximate analysis developed by Lo (Reference 6). His method of solution employs a combined point matching and least square technique. Specific numerical results for $\bar{N}_x$ at several points of a plate of aspect ratio $\lambda = 1.2$ and $\nu = 0.3$ have been extracted from Lo's data and compared with the corresponding computer calculations in Table II. Also shown are the results for $\bar{N}_y$. The function N_T used in calculations have been chosen to be

$$N_T = \frac{Eh^2}{b^3(1-\nu)} x(y - 4x) \quad . \tag{73}$$

This is one of many functions which automatically satisfies Equation (72).

The series solution of Equations (49) has been evaluated for 9, 25, and 36 terms. The table shows that the nondimensional stress resultants thus obtained have apparently converged to accurate results after 9 terms. The values of $\bar{N}_x$ obtained from Reference 6 agree well with these results.

D. CASE IV: CLAMPED PLATE

A test program for the clamped plate is again obtained from Reference 6 where numerical results are given for the case of uniform pressure loading. This case is analogous to a thermal bending problem if we set

$$\nabla^2 M_T = \text{constant} \tag{74}$$

in the deflection equilibrium equation (13). For purposes of comparison we select

$$M_T = \frac{(1-\nu)\,Dh}{b^2}\left(\frac{x^2}{a^2} + \frac{2y^2}{b^2}\right) \tag{75}$$

which satisfies Equation (74). In Table III the computer calculations are compared with Lo's approximate values for $\lambda = 1.2$ and $\nu = 0.3$. As in Case III, the series solutions converge rapidly and substantiate Lo's results.

E. CASE V: SIMPLY SUPPORTED PLATE

The Fourier series solution for the deflections $\bar{w}$ given by Equation (54) will generally converge rapidly. The bending moments, which involve second derivatives of the deflection function, must be evaluated from the slowly converging Fourier series of Equations (55). However, for the special case $\bar{M}_T$ = constant, the bending moments may be evaluated from a modified series which converges more rapidly (References 1 and 7). Numerical results are obtained on this basis in Reference 1 for a number of aspect ratios. Therefore, the more general solution procedure of the present study has been tested against these results. The data of Table IV show this comparison when $\bar{M}_T = 1$, $\lambda = 0.5$, and $\nu = 0.3$. The number of

terms taken are 2500, 3600, and 6400. As expected, the results for the deflection converge very rapidly. Actually, the number of terms required for accurate deflections is considerably less than the 2500 terms taken. The convergence of the bending moments is slower and oscillatory in nature. Nevertheless, the bending moments $\bar{M}_y$ in the long direction, which are generally much larger than $\bar{M}_x$ in the plate interior, differ from the results of Reference 1 by at most 4% after only 2500 terms have been evaluated. Further, the maximum discrepancy between the data is reduced to 2.5% after 6400 terms. We note that the values of $\bar{M}_x$ and $\bar{M}_y$ computed from Equations (55) both deviate in magnitude from those of Reference 1 by approximately the same amount. This results in a larger relative discrepancy in $\bar{M}_x$, which is not too significant, however, since $\bar{M}_x$ is much smaller than $\bar{M}_y$ in the plate interior.

TABLE II

CASE III: COMPARISON OF COMPUTER CALCULATIONS WITH PREVIOUS APPROXIMATE RESULTS

η \ ξ	0	1/6	1/3	1/2	Number of Terms in Series (49)
	$\overline{N}_x$				
0	0	.204	.433	.511	9
	0	.204	.433	.511	25
	0	.204	.434	.512	36
	0	.203	.432	.512	Ref. 6
1/6	0	.013	.038	.050	9
	0	.013	.038	.050	25
	0	.013	.038	.050	36
	0	--	--	--	Ref. 6
1/3	0	-.056	-.124	-.150	9
	0	-.056	-.124	-.150	25
	0	-.055	-.124	-.150	36
	0	--	--	--	Ref. 6
1/2	0	-.071	-.166	-.203	9
	0	-.071	-.166	-.203	25
	0	-.071	-.166	-.203	36
	0	-.071	-.164	-.203	Ref. 6
	$\overline{N}_y$				
0	0	0	0	0	9
	0	0	0	0	25
	0	0	0	0	36
1/6	.1557	-.0018	-.0357	-.0370	9
	.1596	-.0021	-.0351	-.0378	25
	.1591	-.0021	-.0351	-.0377	36
1/3	.3592	.0024	-.0863	-.0949	9
	.3641	.0022	-.0854	-.0963	25
	.3643	.0025	-.0855	-.0963	36
1/2	.4380	.0059	-.1070	-.1202	9
	.4433	.0058	-.1060	-.1218	25
	.44[illegible]	.0056	-.1059	-.1219	36

TABLE III

CASE IV: COMPARISON OF COMPUTER CALCULATIONS WITH PREVIOUS APPROXIMATE RESULTS

η \ ξ	0	1/6	1/3	1/2	Number of Terms in Series (51)
			$\bar{\bar{w}}$		
0	0	0	0	0	9
	0	0	0	0	25
	0	0	0	0	36
	0	0	0	0	Ref. 6
1/6	0	-.00117	-.00257	-.00307	9
	0	-.00117	-.00257	-.00307	25
	0	-.00117	-.00257	-.00307	36
	0	---	---	-.00301	Ref. 6
1/3	0	-.00277	-.00620	-.00747	9
	0	-.00277	-.00620	-.00747	25
	0	-.00277	-.00620	-.00747	36
	0	---	---	-.00745	Ref. 6
1/2	0	-.00341	-.00769	-.00929	9
	0	-.00341	-.00769	-.00929	25
	0	-.00341	-.00768	-.00929	36
	0	---	---	-.00927	Ref. 6
			$\bar{\bar{M}}_x$		
0	0	.0134	-.0236	-.1468	9
	0	.0136	-.0236	-.1465	25
	0	.0136	-.0234	-.1466	36
	0	---	---	---	Ref. 6
1/6	.0493	-.0820	-.1831	-.3204	9
	.0519	-.0822	-.1826	-.3210	25
	.0517	-.0823	-.1826	-.3211	36
	---	---	---	---	Ref. 6
1/3	.0197	-.2596	-.4166	-.5664	9
	.0230	-.2600	-.4159	-.5674	25
	.0231	-.2595	-.4161	-.5673	36
	---	---	---	---	Ref. 6
1/2	-.2050	-.5380	-.7166	-.8720	9
	-.2014	-.5382	-.7161	-.8731	25
	-.2005	-.5383	-.7159	-.8732	36
	-.206	-.533	-.715	-.873	Ref. 6

TABLE III (Continued)

CASE IV: COMPARISON OF COMPUTER CALCULATIONS WITH PREVIOUS APPROXIMATE RESULTS

η \ ξ	0	1/6	1/3	1/2	Number of Terms in Series (51)
			$\bar{\bar{M}}_y$		
0	0	.1094	.1806	.0941	9
	0	.1102	.1813	.0950	25
	0	.1101	.1800	.0950	36
	0	---	---	.0943	Ref. 6
1/6	-.0241	-.0751	-.1486	-.2796	9
	-.0233	-.0753	-.1483	-.2799	25
	-.0234	-.0755	-.1482	-.2798	36
	---	---	---	-.280	Ref. 6
1/3	-.1496	-.2870	-.4345	-.5922	9
	-.1486	-.2868	-.4341	-.5925	25
	-.1486	-.2866	-.4343	-.5925	36
	---	---	---	-.592	Ref. 6
1/2	-.4115	-.5742	-.7443	-.9111	9
	-.4104	-.5742	-.7443	-.9116	25
	-.4102	-.5745	-.7442	-.9116	36
	---	---	---	-.9116	Ref. 6

TABLE IV

CASE V. COMPARISON OF COMPUTER CALCULATIONS WITH RESULTS OF REFERENCE 1

η \ ξ	0	1/6	1/3	1/2	Number of Terms in Series (54)
			$\bar{w}$		
0	0	0	0	0	2500
	0	0	0	0	3600
	0	0	0	0	6400
	0	0	0	0	Ref. 1
1/6	0	.0116	.0178	.0198	2500
	0	.0116	.0178	.0198	3600
	0	.0116	.0178	.0198	6400
	0	.0116	.0178	.0198	Ref. 1
1/3	0	.0151	.0239	.0268	2500
	0	.0151	.0239	.0268	3600
	0	.0151	.0239	.0268	6400
	0	.0151	.0239	.0268	Ref. 1
1/2	0	.0160	.0254	.0285	2500
	0	.0160	.0254	.0285	3600
	0	.0160	.0254	.0285	6400
	0	.0160	.0254	.0285	Ref. 1

η \ ξ	0	1/6	1/3	1/2	Number of Terms in Series (55)
			$\bar{M}_x$		
0	0	-.700	-.700	-.700	2500
	0	-.700	-.700	-.700	3600
	0	-.700	-.700	-.700	6400
	0	-.700	-.700	-.700	Ref. 1
1/6	0	-.189	-.271	-.296	2500
	0	-.199	-.292	-.322	3600
	0	-.161	-.267	-.310	6400
	0	-.168	-.280	-.302	Ref. 1
1/3	0	-.073	-.097	-.108	2500
	0	-.087	-.122	-.137	3600
	0	-.052	-.101	-.129	6400
	0	-.062	-.109	-.123	Ref. 1
1/2	0	-.048	-.055	-.060	2500
	0	-.063	-.082	-.090	3600
	0	-.03'	-.064	-.087	6400
	0	-.040	-.067	-.079	Ref. 1

TABLE IV (Continued)

CASE V: COMPARISON OF COMPUTER CALCULATIONS WITH RESULTS OF REFERENCE 1

η \ ξ	0	1/6	1/3	1/2	Number of Terms in Series (55)
			$\bar{M}_y$		
0	0	0	0	0	2500
	0	0	0	0	3600
	0	0	0	0	6400
	0	0	0	0	Ref. 1
1/6	-.700	-.546	-.438	-.405	2500
	-.700	-.556	-.451	-.419	3600
	-.700	-.518	-.417	-.389	6400
	-.700	-.532	-.420	-.398	Ref. 1
1/3	-.700	-.635	-.584	-.566	2500
	-.700	-.656	-.609	-.593	3600
	-.700	-.631	-.588	-.575	6400
	-.700	-.638	-.591	-.577	Ref. 1
1/2	-.700	-.653	-.618	-.606	2500
	-.700	-.678	-.648	-.637	3600
	-.700	-.667	-.640	-.633	6400
	-.700	-.660	-.633	-.621	Ref. 1

SECTION VII. SAMPLE PROBLEM - HEAT TRANSFER AND THERMAL STRESS CALCULATIONS FOR AN AERODYNAMICALLY H' ATED WINDSHIELD

The computer program has been applied to the problem of determining the temperatures, thermal stresses, and deflections in a rectangular glass plate subject to time- and space-dependent surface heating. In the specification of the geometry, boundary conditions, and heating environment, an attempt has been made to reasonably simulate the conditions encountered in an X-15 type windshield.

The chosen plate geometry and material properties are:

$a = 32.0$ in.

$b = 8.4$ in.

$h = .375$ in.

$E = 12.45 \times 10^{6}$ lb/in.^{2}

$\nu = .26$

$\alpha = 25.5 \times 10^{-7}$ in./in. -°F

$\frac{K}{\rho c} = .795 \times 10^{-3}$ in.^{2}/sec

where the last quantity is also referred to as the thermal diffusivity. The material properties are listed for a #1723 fine-annealed aluminosilicate glass at representative temperatures.

In order to approximate the boundary restraints due to the windshield framing, Cases II and V are assumed to be applicable. This implies that the plate edges are free to slide and rotate within the frame while all other displacements are prevented. The edges of the plate are assumed to be perfectly insulated, while the temperatures of the faces, i.e., $T(\xi, \eta, \frac{h}{2}, t)$ and $T(\xi, \eta, -\frac{h}{2}, t)$ are prescribed. Here the interior face is cooled so that a constant temperature rise of 150°F is maintained, viz.,

$$T(\xi, \eta, \frac{h}{2}, t) \equiv 150°F .$$

The face exposed to the airstream $(z = -\frac{h}{2})$ is aerodynamically heated, which results in a surface temperature distribution which varies timewise according to

$$T(\xi, \eta, -\frac{h}{2}, t) = 150 + T_o(\xi, \eta)\, f(t)$$

where $f(t)$ is defined by the following sketch.

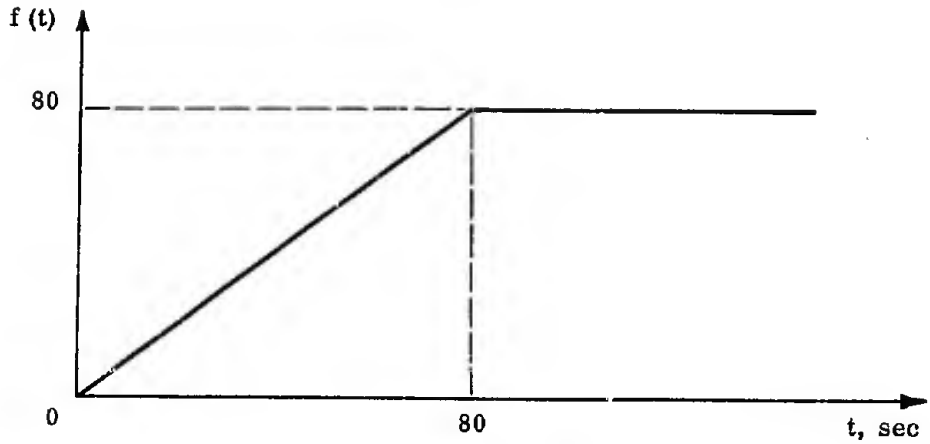

Thus the temperature rise on the hot face increases linearly for 80 seconds, and remains constant thereafter. The function $T_o(\xi, \eta)$, which defines the space variation of the temperature rise, is given by

$$T_o(\xi,\eta) = \begin{cases} \frac{45}{8} + 5\left(\eta - \frac{1}{2}\right)^2 & ; \ 0 \le \xi \le \frac{7}{8} \\ \frac{45}{8} + \frac{5}{4}\left[(2\eta - 1)^2 + 4(8\xi - 7)^2 \right. & \\ \quad \left. + (8\xi - 7)^2 (2\eta - 1)^2\right] & ; \ \frac{7}{8} \le \xi \le 1 \ . \end{cases} \tag{76}$$

The graph of this function is shown for three sections of the plate in Figure 4. Note that the temperature rises sharply in the neighborhood of the edge $\xi = 1$. This variation was chosen to simulate the stagnation condition which would occur at the aft edge of the windshield because of the tripping of the airstream by a retaining strip.

The above data were entered into the computer program and numerical solutions were obtained at grid points which divided the plate into ten, four, and six equal intervals in the ξ, η, and z directions, respectively. This resulted in an evaluation of the temperatures, stresses, and deflections at 385 points for several time slices.

The temperatures at all grid points were determined at two-second intervals from time $t = 0$ to $t = 80$ sec. Also, the steady-state temperature distribution was calculated. An inspection of these data clearly revealed that maximum stresses and deflections would occur either at the end of the heating ramp (i.e., at $t = 80$ sec) or in the steady-state condition. Therefore, the stress analysis was performed for these two heated states. In addition, in order to demonstrate the plate response at an early stage of the heating process, stresses and deflections were calculated at $t = 4$ sec. Temperature variations through the thickness at the center of the plate (which are typical of the thickness variations elsewhere) are shown in Figure 5. Note that the steady-state condition is typified by an essentially linear gradient in the z direction, implying negligible heat flow over the planform. Since the heating is symmetrical about the long centerline of the plate ($\eta = .5$), the calculated quantities also possess this symmetry.

The deflections along the plate centerlines are shown in Figure 6. The deflections along the centerline $\eta = .5$ tend to become constant in the plate interior, and drop off sharply in the neighborhood of the edges $\xi = 0$ and $\xi = 1$. This effect is less pronounced in the short direction, indicating that (because of the large aspect ratio) the plate deflection is characterized by the thermal bending of independent strips in the η direction.

Stress variations through thickness are shown at three planform points in Figure 7. The trends indicated by this figure are typical of what occurs throughout the plate, namely that the peak stresses for all time slices occur either at one of the plate faces or in the vicinity of the middle plane. In addition, the steady state stresses are essentially linear through the thickness and are generally larger in magnitude than the transient stresses. Detailed values of the middle plane and face stresses in the x and y directions, for time $t = 80$ sec and the steady-state condition, are given in Figures 8 through 11. The shearing stresses σ_{xy} were found to be negligibly small and are therefore not shown. In general, the stresses acting at the hot face are larger in magnitude than those at the cold face. Note that because of the sharp rise in temperature near the edge $\xi = 1$, the stresses rapidly change from compression to tension as the edge is approached.

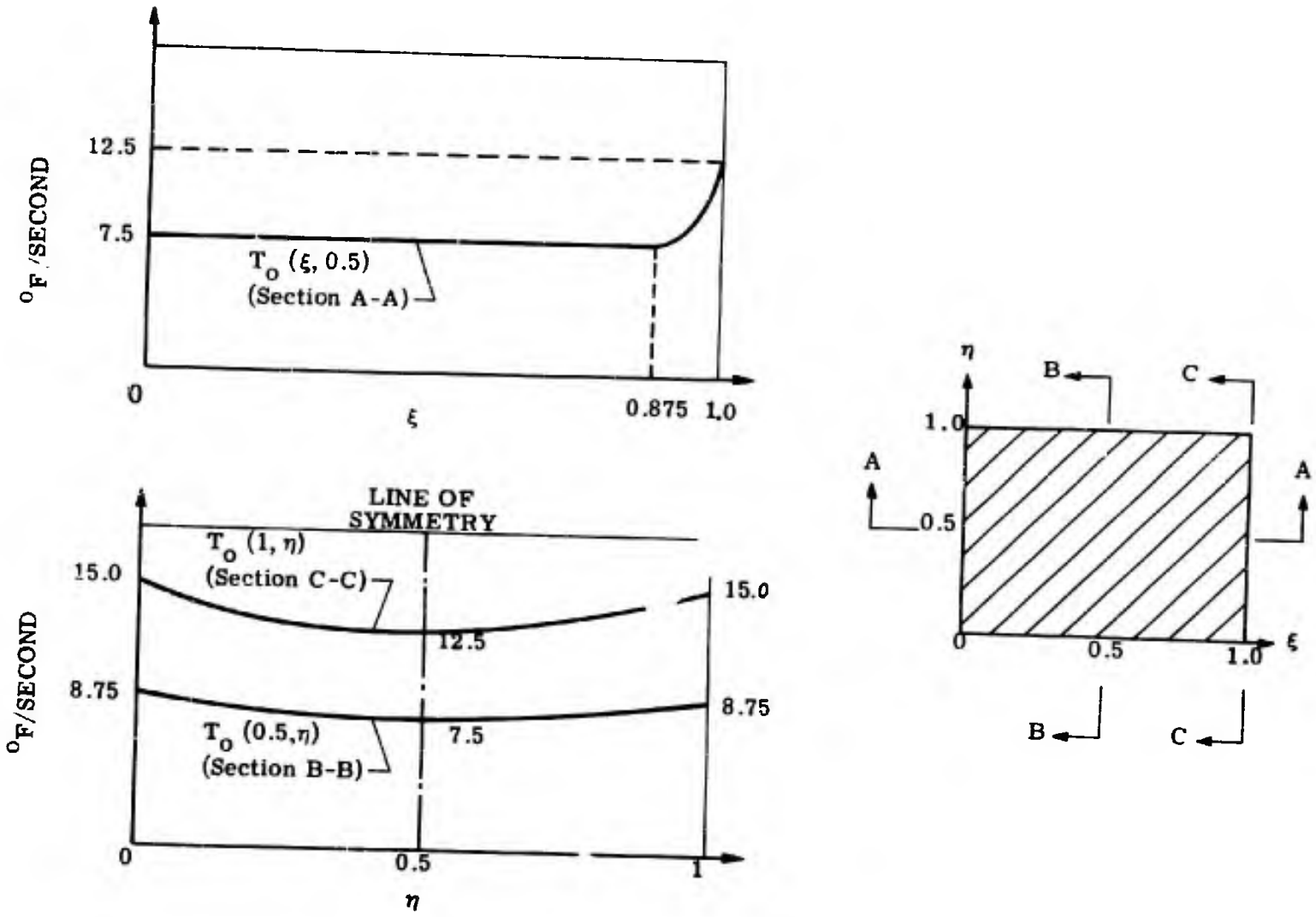

Figure 4. Temperature Variation on the Hot Face

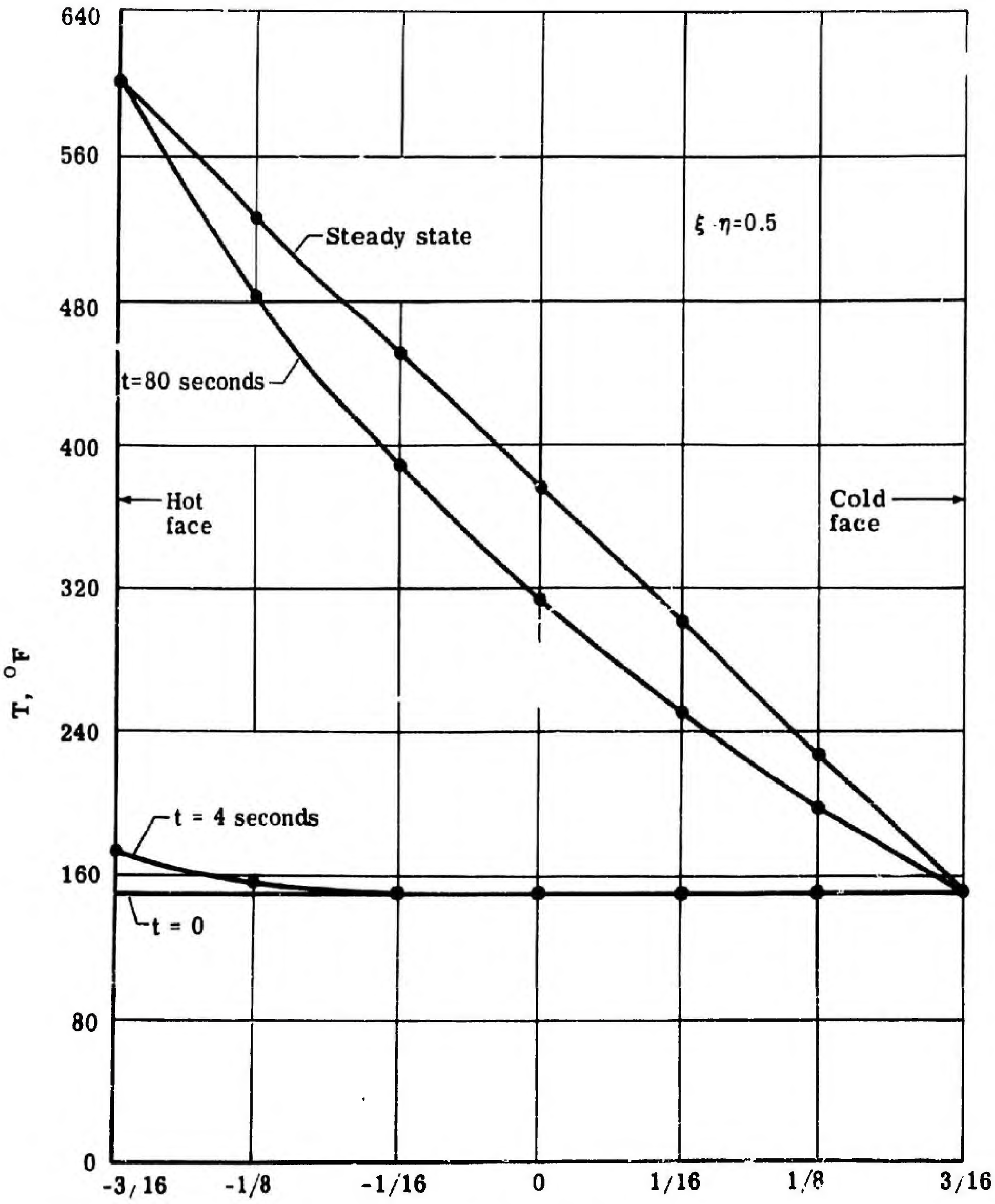

Figure 5. Variation of Temperature Through the Thickness at Plate Center; t = 0, 4, 80 Seconds and Steady State

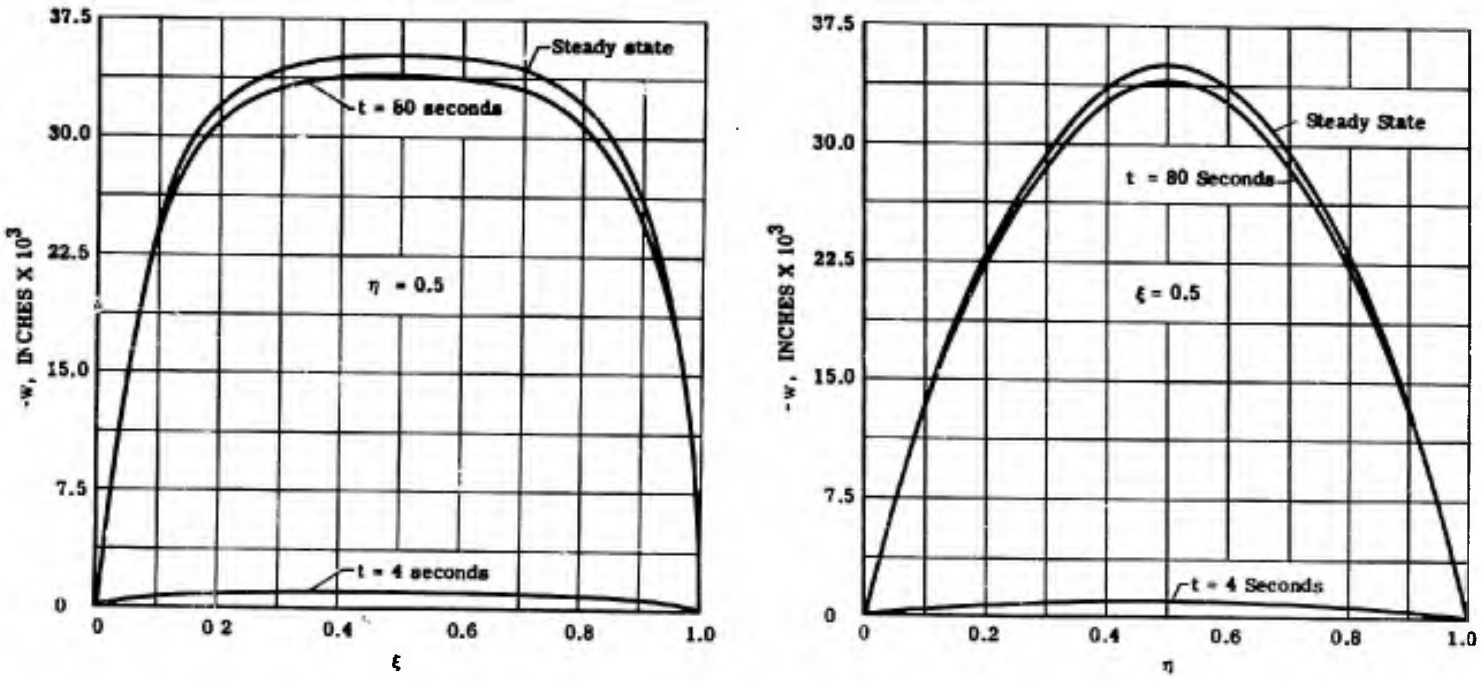

Figure 6. Centerline Deflections at t = 4, 80 Seconds and Steady State

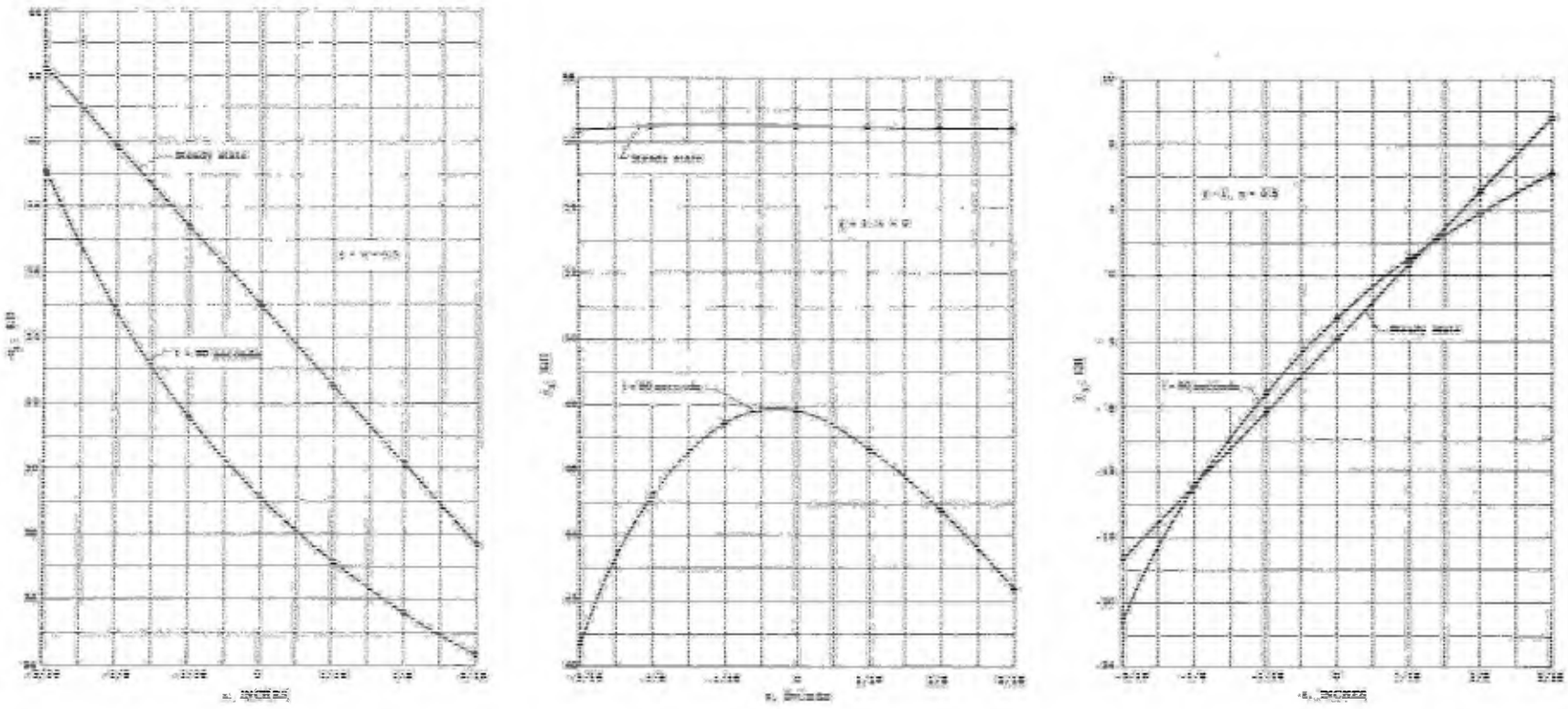

Figure 7. Typical Stress Variations Through the Thickness for t = 80 Seconds and Steady State

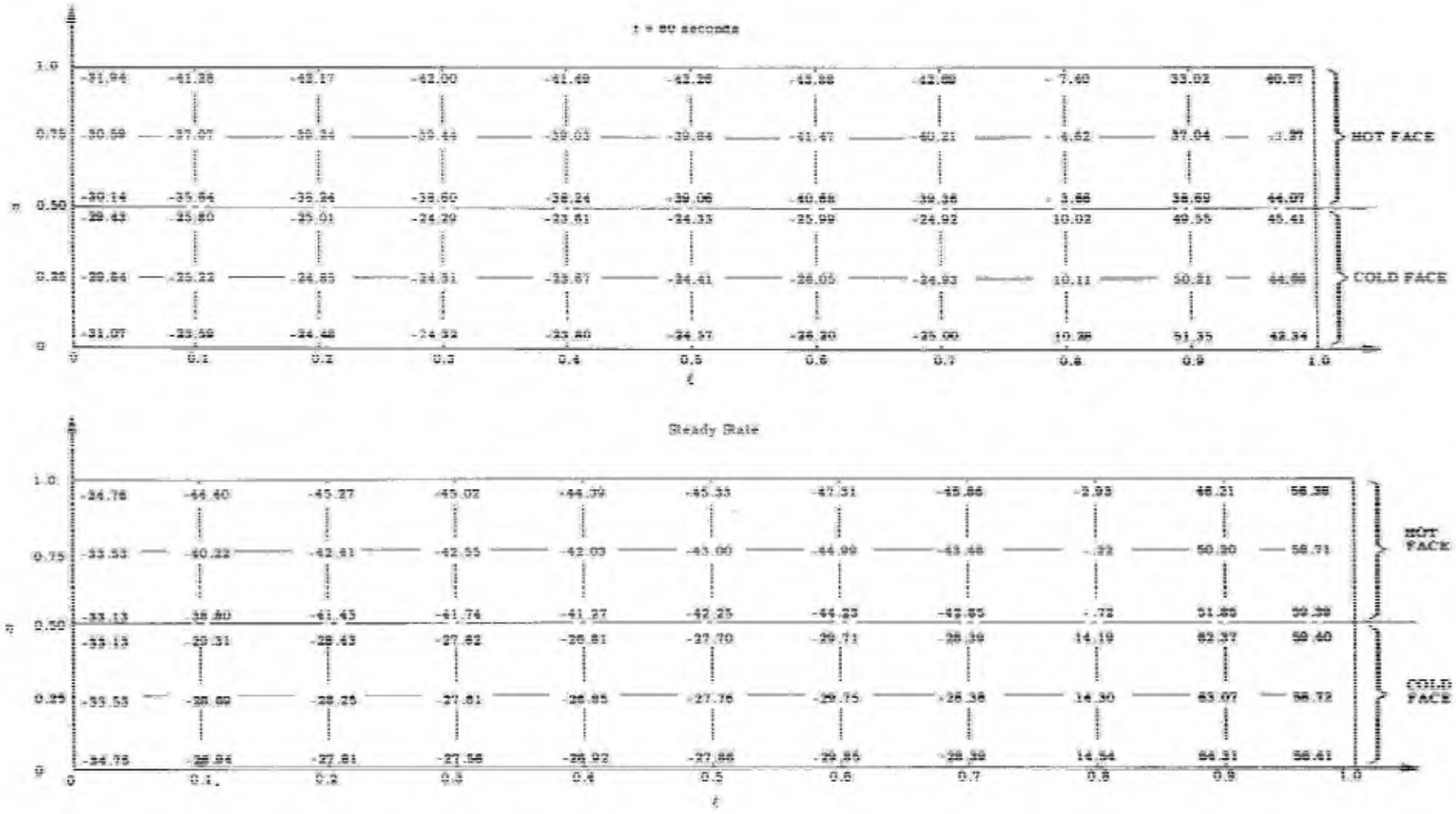

Figure 8. σ_x(KSI) at Plate Faces; t = 80 Seconds and Steady State

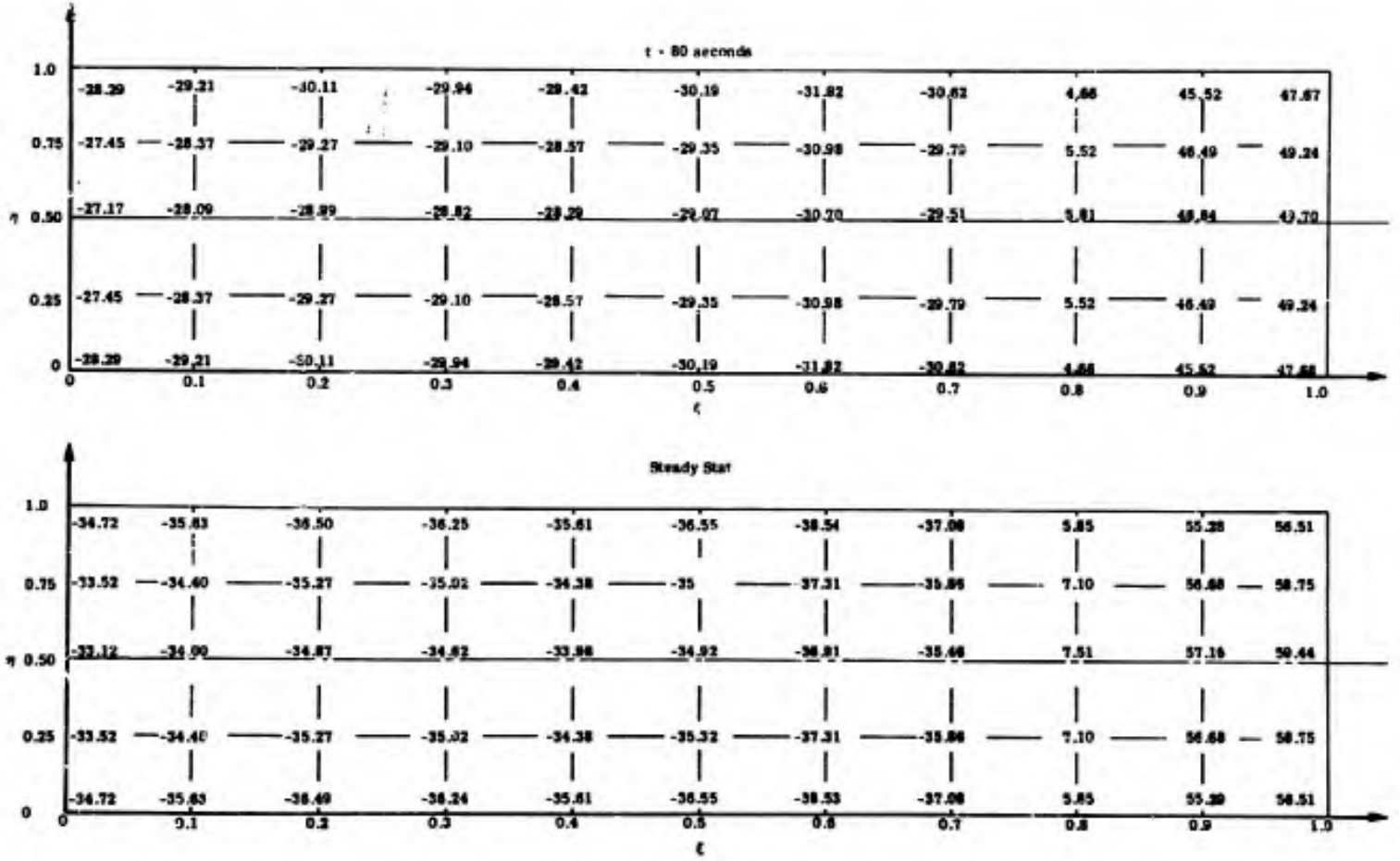

Figure 9. σ_x(KSI) at the Middle Plane, t = 80 Seconds and Steady State

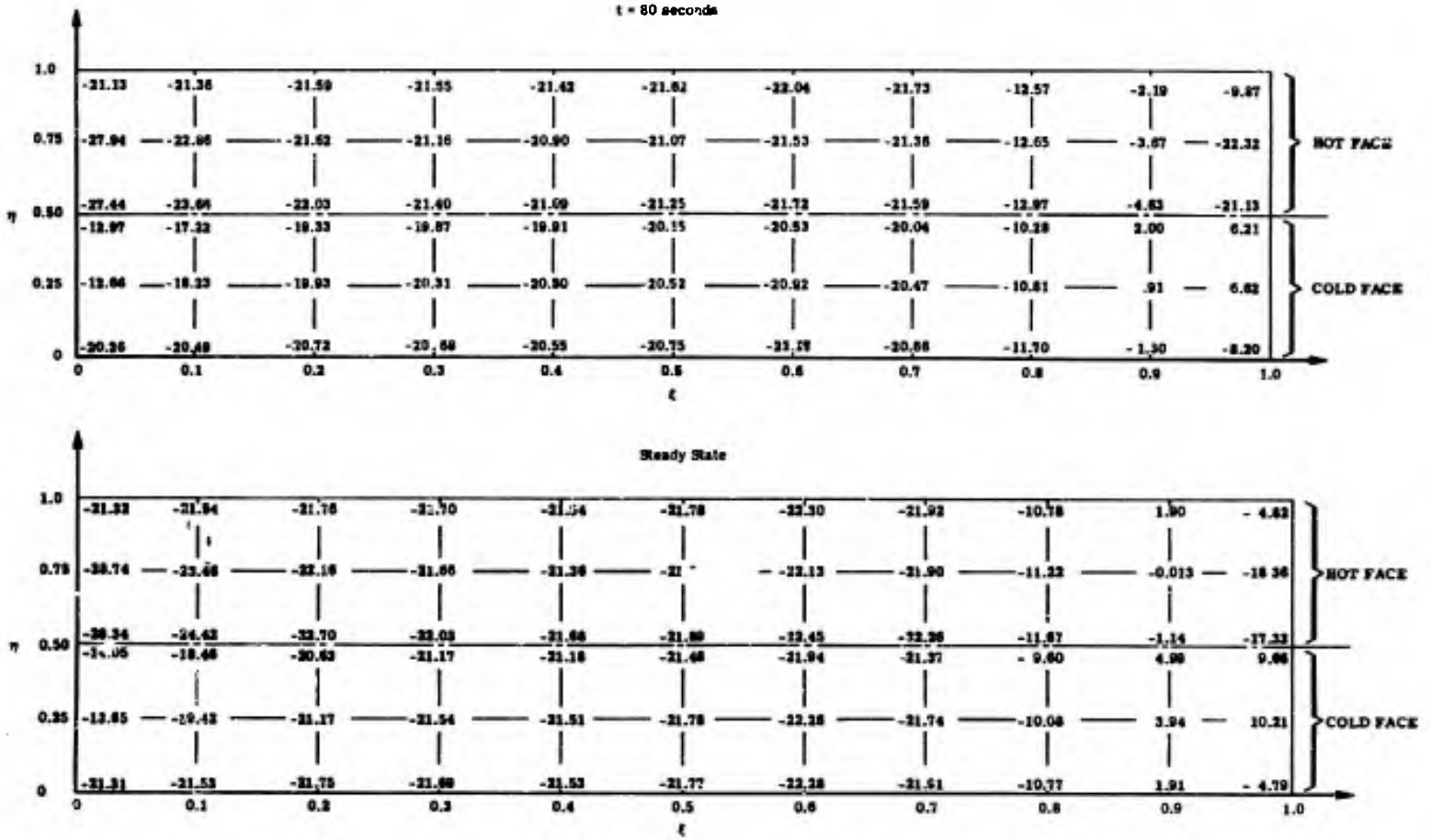

Figure 10. σ_y (KSI) at Plate Faces; t = 80 Seconds and Steady State

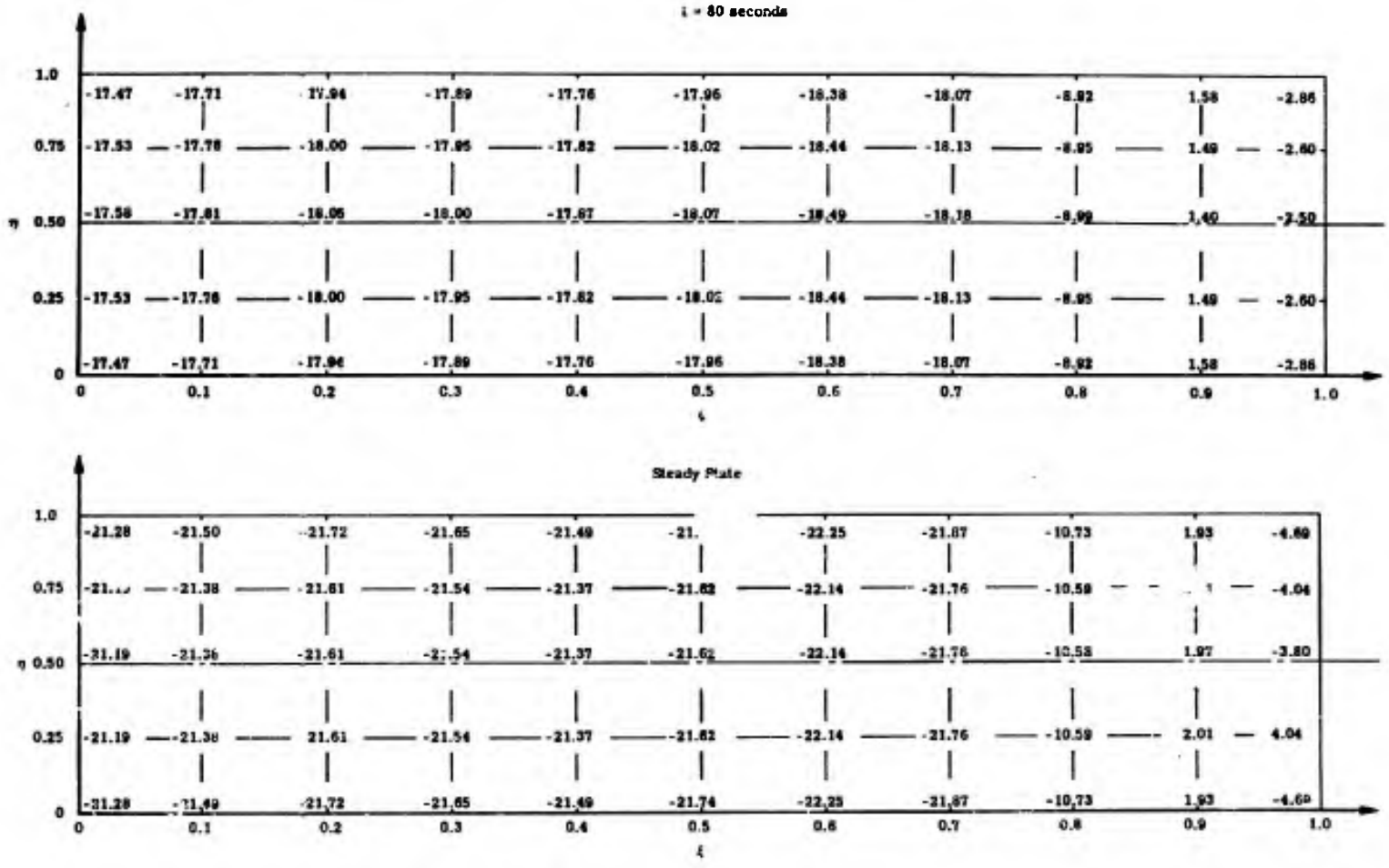

Figure 11. σ_y(KSI) at the Middle Plane; t = 80 Seconds and Steady State

SECTION VIII - REFERENCES

1. Forray, M.J., Newman, M. and Kossar, J., "Thermal Stresses and Deflections in Rectangular Panels, Part I - The Analysis and Test of Rectangular Panels with Temperature Gradients Through the Thickness," ASD-TR-61-537, Republic Aviation Corporation Report RAC 548 (ARD-688-6), November 1961.

2. Boley, B.A. and Weiner, J.H., "Theory of Thermal Stresses," John Wiley and Sons, Inc., 1960, pp 260-261.

3. Hildebrand, F.B., "Methods of Applied Mathematics," Prentice-Hall, Inc., 1952, pp 185-187.

4. Jeffreys, H. and Jeffreys, B.S., "Mathematical Physics," Cambridge, 3rd Edition, 1956, p 365.

5. Salvadori, M.G. and Baron, M.L., "Numerical Methods in Engineering," Prentice-Hall, Inc., 1952, pp 23-28.

6. Lo, Chunchang, "Bending of Rectangular Plates with all Edges Clamped," Master of Science Thesis, The Ohio State University, 1960.

7. Timoshenko, S., "Theory of Plates and Shells," First Edition, McGraw Hill Book Co., Inc., 1940, pp 176-180.

Aeronautical Systems Division, Dir/Aeromechanics, Flight Dynamics Laboratory, Wright-Patterson AFB, Ohio. Rpt Nr ASD-TR-61-537, Pt II. THERMAL STRESSES AND DEFLECTIONS IN RECTANGULAR PANELS: The Analysis of Rectangular Panels with Three-Dimensional Heat Inputs. Final Report, Oct 62, 48 p. incl illus., tables, 7 refs.

Unclassified Report

The linear thermal stress problem of a rectangular plate subjected to arbitrary three-dimensional heating is solved. Analytic solutions for the determination of deflections and stresses are presented for several types of boundary conditions. A digital computer program is developed which, starting with heat transfer, material and geometry data, yields a numerical evaluation of transient temperatures, quasi-static deflections, and stresses. A copy of this report may be obtained by contacting the Flight Dynamics Laboratory, ASRMDS-22.

UNCLASSIFIED

1. Equations
2. Thermal stresses
3. Computer program
I. AFSC Project 1467, Task 146702
II. Contract AF33(616)-7751
III. Republic Aviation Corp. Farmingdale, L.I., N.Y.
IV. M. Newman
M.J. Forray
V. RAC 548-1(ARD-688-7)
VI. Not aval fr OTS
VII. In ASTIA collection

UNCLASSIFIED

Aeronautical Systems Division, Dir/Aeromechanics, Flight Dynamics Laboratory, Wright-Patterson AFB, Ohio. Rpt Nr ASD-TR-61-537, Pt II. THERMAL STRESSES AND DEFLECTIONS IN RECTANGULAR PANELS: The Analysis of Rectangular Panels with Three-Dimensional Heat Inputs. Final Report, Oct 62, 48 p. incl illus., tables, 7 refs.

Unclassified Report

The linear thermal stress problem of a rectangular plate subjected to arbitrary three-dimensional heating is solved. Analytic solutions for the determination of deflections and stresses are presented for several types of boundary conditions. A digital computer program is developed which, starting with heat transfer, material and geometry data, yields a numerical evaluation of transient temperatures, quasi-static deflections, and stresses. A copy of this report may be obtained by contacting the Flight Dynamics Laboratory, ASRMDS-22.

UNCLASSIFIED

1. Equations
2. Thermal stresses
3. Computer program
I. AFSC Project 1467, Task 146702
II. Contract AF33(616)-7751
III. Republic Aviation Corp. Farmingdale, L.I., N.Y.
IV. M. Newman
M.J. Forray
V. RAC 548-1(ARD-688-7)
VI. Not aval fr OTS
VII. In ASTIA collection

UNCLASSIFIED

Aeronautical Systems Division, Dir/Aeromechanics, Flight Dynamics Laboratory, Wright-Patterson AFB, Ohio. Rpt Nr ASD-TR-61-537, Pt II. THERMAL STRESSES AND DEFLECTIONS IN RECTANGULAR PANELS: The Analysis of Rectangular Panels with Three-Dimensional Heat Inputs. Final Report, Oct 62, 48 p. incl illus., tables, 7 refs.

Unclassified Report

The linear thermal stress problem of a rectangular plate subjected to arbitrary three-dimensional heating is solved. Analytic solutions for the determination of deflections and stresses are presented for several types of boundary conditions. A digital computer program is developed which, starting with heat transfer, material and geometry data, yields a numerical evaluation of transient temperatures, quasi-static deflections, and stresses. A copy of this report may be obtained by contacting the Flight Dynamics Laboratory, ASRMDS-22.

UNCLASSIFIED

this report may be obtained by contacting the Flight Dynamics Laboratory, ASRMDS-22.

1. Equations
2. Thermal stresses
3. Computer program
I. AFSC Project 1467, Task 146702
II. Contract AF33(616)-7751
III. Republic Aviation Corp. Farmingdale, L.I., N.Y.
IV. M. Newman
M.J. Forray
V. RAC 548-1(ARD-688-7)
VI. Not aval fr OTS
VII. In ASTIA collection

UNCLASSIFIED

UNCLASSIFIED

Aeronautical Systems Division, Dir/Aeromechanics, Flight Dynamics Laboratory, Wright-Patterson AFB, Ohio. Rpt Nr ASD-TR-61-537, Pt II. THERMAL STRESSES AND DEFLECTIONS IN RECTANGULAR PANELS: The Analysis of Rectangular Panels with Three-Dimensional Heat Inputs. Final Report Oct 62, 48 p. incl illus., tables, 7 refs.

Unclassified Report

The linear thermal stress problem of a rectangular plate subjected to arbitrary three-dimensional heating is solved. Analytic solutions for the determination of deflections and stresses are presented for several types of boundary conditions. A digital computer program is developed which, starting with heat transfer, material and geometry data, yields a numerical evaluation of transient temperatures, quasi-static deflections, and stresses. A copy of this report may be obtained by contacting the Flight Dynamics Laboratory, ASRMDS-22.

this report may be obtained by contacting the Flight Dynamics Laboratory, ASRMDS-22.

UNCLASSIFIED

1. Equations
2. Thermal stresses
3. Computer program
I. AFSC Project 1467, Task 146702
II. Contract AF33(616)-7751
III. Republic Aviation Corp. Farmingdale, L.I., N.Y.
IV. M. Newman
M.J. Forray
V. RAC 548-1(ARD-688-7)
VI. Not aval fr OTS
VII. In ASTIA collection

UNCLASSIFIED

UNCLASSIFIED

Aeronautical Systems Division, Dir/Aeromechanics, Flight Dynamics Laboratory, Wright-Patterson AFB, Ohio. Rpt Nr ASD-TR-61-537, Pt II. THERMAL STRESSES AND DEFLECTIONS IN RECTANGULAR PANELS: The Analysis of Rectangular Panels with Three-Dimensional Heat Inputs. Final Report, Oct 62, 48 p. incl illus., tables, 7 refs.

Unclassified Report

The linear thermal stress problem of a rectangular plate subjected to arbitrary three-dimensional heating is solved. Analytic solutions for the determination of deflections and stresses are presented for several types of boundary conditions. A digital computer program is developed which, starting with heat transfer, material and geometry data, yields a numerical evaluation of transient temperatures, quasi-static deflections, and stresses. A copy of this report may be obtained by contacting the Flight Dynamics Laboratory, ASRMDS-22

UNCLASSIFIED

1. Equations
2. Thermal stresses
3. Computer program
   I. AFSC Project 1467, Task 146702
   II. Contract AF33(616)-7751
   III. Republic Aviation Corp. Farmingdale, L.I., N.Y.
   IV. M. Newman M.J. Forray
   V. RAC 548-1(ARD-688-7)
   VI. Not aval fr OTS
   VII. In ASTIA collection

UNCLASSIFIED

Aeronautical Systems Division, Dir/Aeromechanics, Flight Dynamics Laboratory, Wright-Patterson AFB, Ohio. Rpt Nr ASD-TR-61-537, Pt II. THERMAL STRESSES AND DEFLECTIONS IN RECTANGULAR PANELS: The Analysis of Rectangular Panels with Three-Dimensional Heat Inputs. Final Report, Oct 62, 48 p. incl illus., tables, 7 refs.

Unclassified Report

The linear thermal stress problem of a rectangular plate subjected to arbitrary three-dimensional heating is solved. Analytic solutions for the determination of deflections and stresses are presented for several types of boundary conditions. A digital computer program is developed which, starting with heat transfer, material and geometry data, yields a numerical evaluation of transient temperatures, quasi-static deflections, and stresses. A copy of this report may be obtained by contacting the Flight Dynamics Laboratory, ASRMDS-22.

UNCLASSIFIED

1. Equations
2. Thermal stresses
3. Computer program
   I. AFSC Project 1467, Task 146702
   II. Contract AF33(616)-7751
   III. Republic Aviation Corp. Farmingdale, L.I., N.Y.
   IV. M. Newman M.J. Forray
   V. RAC 548-1(ARD-688-7)
   VI. Not aval fr OTS
   VII. In ASTIA collection

UNCLASSIFIED

Aeronautical Systems Division, Dir/Aeromechanics, Flight Dynamics Laboratory, Wright-Patterson AFB, Ohio. Rpt Nr ASD-TR-61-537, Pt II. THERMAL STRESSES AND DEFLECTIONS IN RECTANGULAR PANELS: The Analysis of Rectangular Panels with Three-Dimensional Heat Inputs. Final Report, Oct 62, 48 p. incl illus., tables, 7 refs.

Unclassified Report

The linear thermal stress problem of a rectangular plate subjected to arbitrary three-dimensional heating is solved. Analytic solutions for the determination of deflections and stresses are presented for several types of boundary conditions. A digital computer program is developed which, starting with heat transfer, material and geometry data, yields a numerical evaluation of transient temperatures, quasi-static deflections, and stresses. A copy of this report may be obtained by contacting the Flight Dynamics Laboratory, ASRMDS-22.

UNCLASSIFIED

1. Equations
2. Thermal stresses
3. Computer program
   I. AFSC Project 1467, Task 146702
   II. Contract AF33(616)-7751
   III. Republic Aviation Corp. Farmingdale, L.I., N.Y.
   IV. M. Newman M.J. Forray
   V. RAC 548-1(ARD-688-7)
   VI. Not aval fr OTS
   VII. In ASTIA collection

UNCLASSIFIED

UNCLASSIFIED